In Silico ADME, binding affinities, and properties of synthetic and natural cannabinoid analogs

Maite L. Docampo-Palacios*[^], Giovanni A. Ramirez[^], Tesfay T. Tesfatsion, Monica K. Pittiglio, Kyle P. Ray, Westley Cruces*

[^] Both authors contributed equally. *Corresponding author

Colorado Chromatography Labs, 10505 S. Progress Way Unit 105, Parker CO 80134

Email: wes@coloradochromatography.com, Maite@coloradochromatography.com

Abstract

In recent years, a new set of compounds identified as semi-synthetic cannabinoids have arisen in the market as an alternative to prohibited marijuana or its major natural cannabinoids. These compounds, which are active on the same G protein-coupled receptors (GPCRs) as cannabinoids persist to gain acceptance due to the same cannabinoid-like effects they generate. A dataset of 44 semi-synthetic and natural cannabinoids and their diastereomers were docked using Schrodinger computational software, demonstrating their binding interactions within known binding pockets and domains, predicting their ADME characteristics, p450 estimated sites of metabolism, and hypothesized metabolites.

Keywords: *In silico*, Computational Chemistry, GPCR, Cannabinoids, ADME

1. Introduction

Cannabidiol (CBD) and tetrahydrocannabinol (THC) are the major cannabinoids biosynthesized by *Cannabis sativa;* yet there are cannabinoids to be elucidated within the hundreds of compounds that are naturally biosynthesized. The elucidation of these cannabinoid compounds also promotes the creation of semi- to fully synthetic cannabinoids, to mimic the natural scaffolds and their effects. Recently, a wave of semi-synthetic cannabinoids are beginning to appear in smoke shops and dispensaries both nationally and internationally [1-3]. A growing trend of unqualified personnel performing synthetic chemistry is of concern due to the potential for hazardous byproducts that might remain despite purification [4]. Since their identification in the 1940s [5,6] (Figure 1 and 2), hydrogenated cannabinoids have reappeared within consumer and retail markets as alternative solutions to overtightening regulations and bills in place to limit and restrict cannabinoids derived from hemp or marijuana. Cannabigerol (CBG) and Cannabichromene (CBC), are considered minor constituents within the cannabinoid biome produced by *C. sativa*. CBG is also considered an important precursor to the transformation to CBC, the formation of CBD and THC, through a known biosynthetic pathway (Scheme 1). Harvey et al reported metabolites of tetrahydrocannabigerol (THCBG) and tetrahydrocannabichromene (THCBC) using TMSCl derivatization and GC-MS [14,15]. ElSohly *et al* tested the saturated cannabinoids identifying antimicrobial and antifungal properties [16] which demonstrate that the saturation of CBG and CBC olefins led to an increase in the anti-microbial and anti-fungal characteristics.

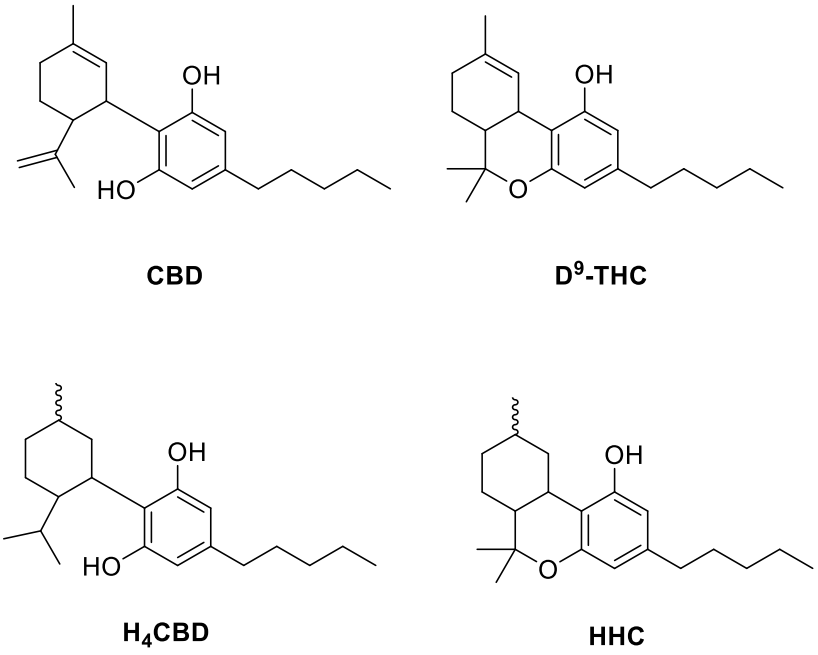

43

44 **Figure 1:** CBD, THC, and their hydrogenated counterparts.

45

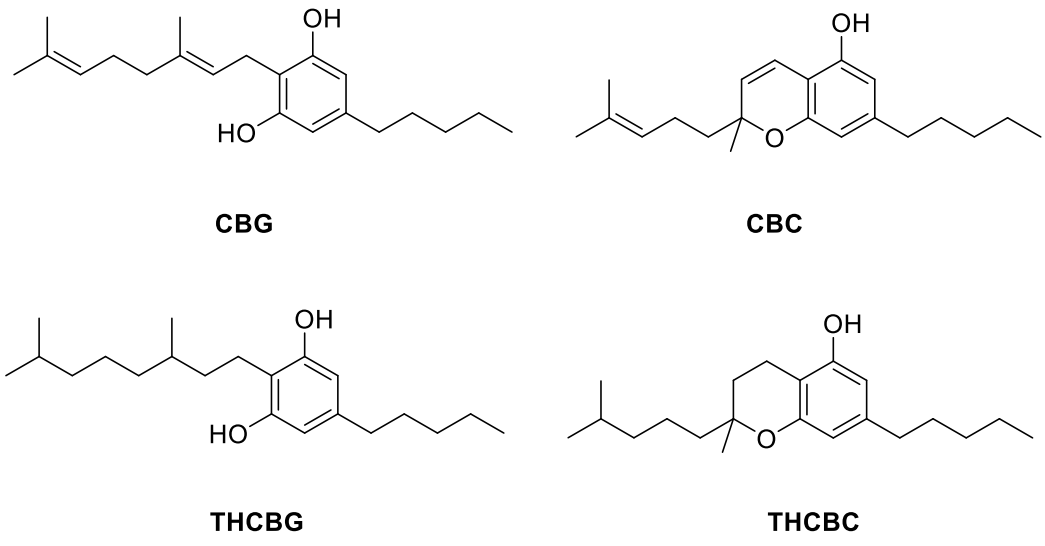

46

47 **Figure 2:** CBG, CBC, and their hydrogenated counterparts.

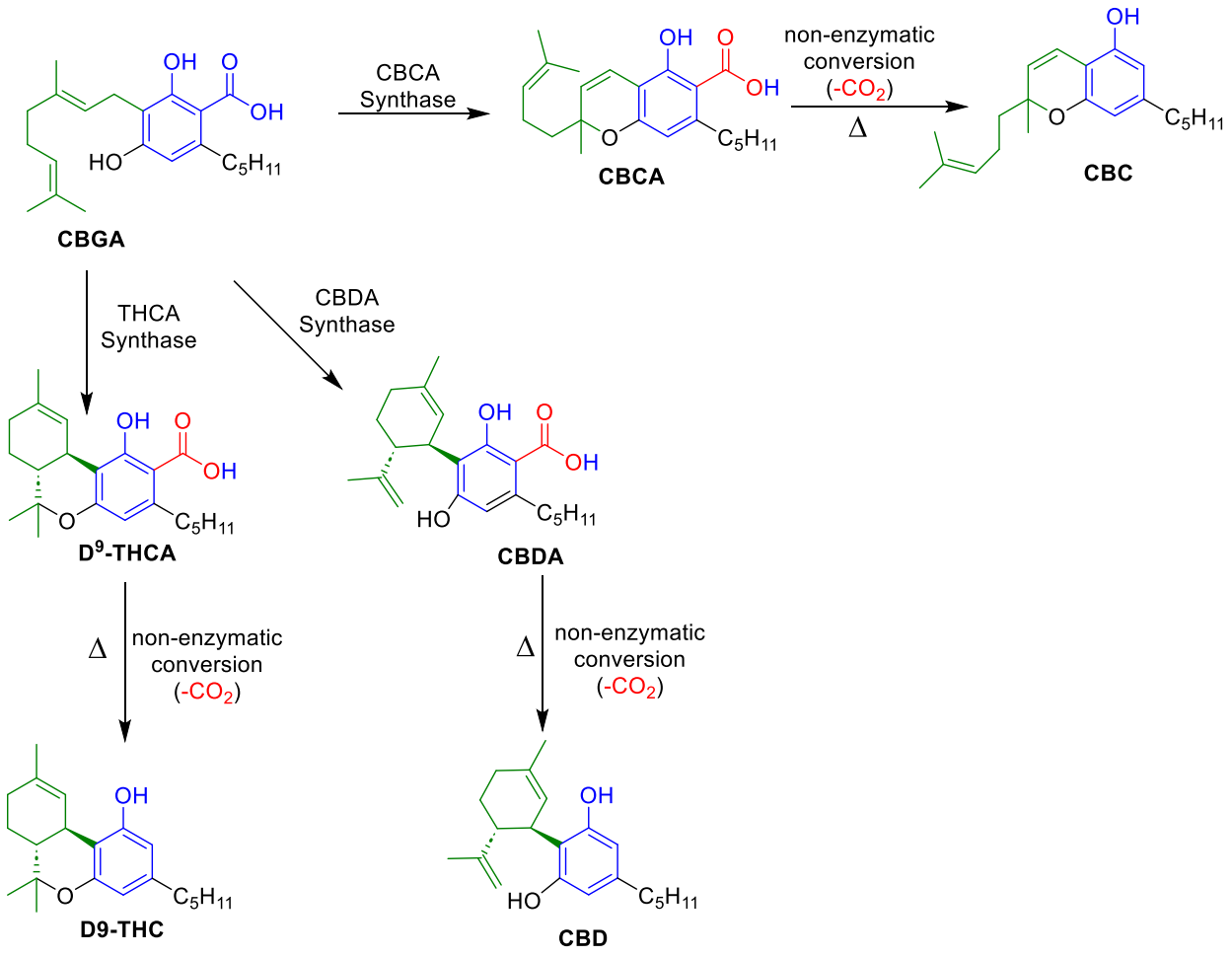

Scheme 1: Biosynthesis of Cannabinoids [17]

Tesfatsion *et al.* demonstrated that saturation of tetrahydrocannabivarin (THCV) to yield hexahydrocannabivarin (HHCV), as shown in Scheme 2, improved IC_{50} values in PANC-1 MTT assays [18].

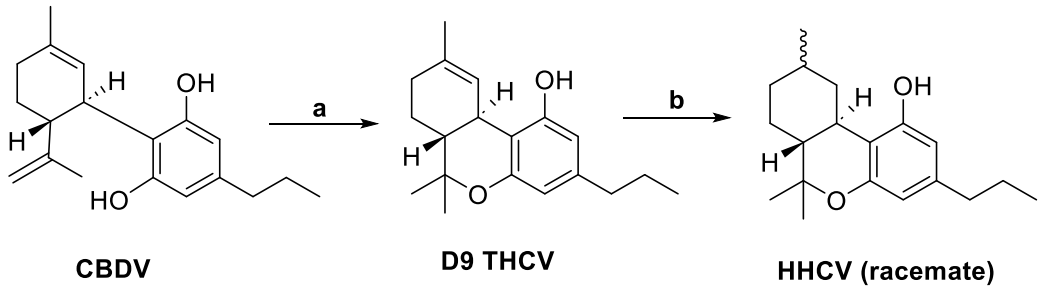

Scheme 2: Synthetic pathway to accomplish HHCV via hydrogenation protocol. Reagents and conditions: (a) DCM, Argon purge 0°C, TIBAL, 0°C-rt, 20 hr.; (1b) EtOH, argon purge, 1hr, rt., Pd/C, 1-5 bar, H_2, 50°C, 24 hr.

Novel Hexahydrocannabinol (HHC) analogs have also shown promise as anticancer agents from cell studies to xenograft models [8, 19-23]. Saturated cannabinoids in the literature have shown promise with medicinal properties [6] compared to their unsaturated counterparts. Lovering *et al*. discussed an increase in saturation or fraction sp^3, and the presence of chiral centers within molecules leads to an increase in the ability for discovery drugs to reach commercialization [24]. The question of where these hydrogenated compounds bind, how they are metabolized, and the nature of their toxicity profiles remains unreported. Using Schrodinger, our group has performed *in-silico* experiments using QikProp, LigPrep, Jaguar, ADMET, Glide, Epik, Desmond, Phase, Protein Preparation Wizard, and sitemap to identify binding interactions and predicted binding scores, predicted ADME, predicted p450 metabolism and metabolites for a series of saturated and non-saturated cannabinoids to compare the difference among these two groups of cannabinoids.

In literature, cannabinoid receptor 1 (CB1) and cannabinoid receptor 2 (CB2) belong within the family of GPCRs [25] and are known to bind with cannabinoids enacting physiological and psychological effects [26]. The use of these receptors focuses on treating diseases, using cannabinoids and similar cannabimimetic compounds, enact agonistic or antagonistic effects, such as anticancer or anti-inflammatory responses when the bound receptors are activated or deactivated [26]. Other receptors were selected due to the similarity of the GPCR family or in relation to the diseases the receptors are implicated in to determine the effects of whether classical cannabinoids or hydrogenated analogs bind within their domains.

Shown below in Figure 3, the protein on the left is Peroxisome proliferator-activated receptor gamma (PPAR-γ) complexed with an indole-based modulator (CID: 11757843). PPAR-γ

is a type II nuclear receptor that functions as a transcription factor [27]. Many agents directly bind and activate PPAR-γ, some include fatty acids and cannabinoids. Activation of PPAR-γ might be responsible in the inhibition of breast, gastric, lung, and prostate cancer cell lines [27,28].

The protein on the right as shown in Figure 3 below is Serine/Threonine-protein kinase (PAK1), a group 1 kinase. PAK1 regulates cytoskeleton remodeling, phenotypic signaling, andgene expression. PAK1 is associated with a wide variety of cellular processes such as, directional motility, invasion, metastasis, growth, cell cycle progression, and angiogenesis [29]. PAK1-signaling-dependent cellular functions regulate both physiologic and disease processes, including cancer, due to overexpression in human cancer [29]. Nikfarjam *et.al.* demonstrated CBD and THC practice their inhibitory effects on pancreatic cancer via a PAK1-dependent pathway, indicating that CBD and THC cancel the Kras protein-activated pathway by affecting PAK1 [30].

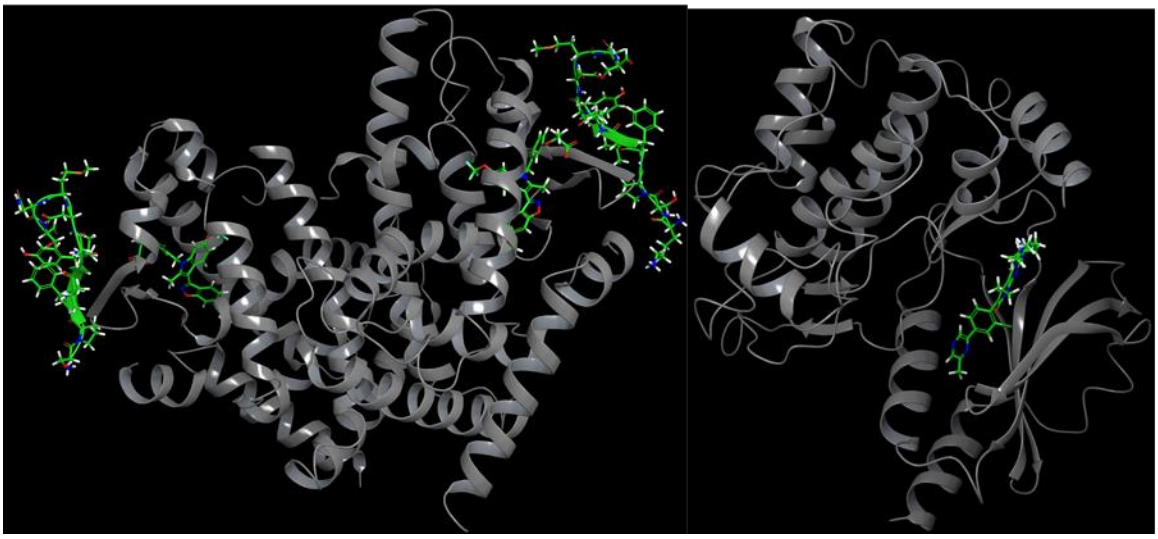

Figure 3: The left protein is the 2P4Y (PPAR-γ complexed with an indole-based modulator). The protein on the right is the 5DFP (PAK1 complexed with inhibitor FRAX1036). Structures were generated from PDB database within Schrödinger maestro.

Several CB1 receptors were chosen as our *in-silico* targets, include 5U09 (Figure 4 left side protein), 6KQI (Figure 5 right side protein), and 7V3Z (Figure 6 right side protein). A protein with no conformational changes was used to dock the ligands compared to a protein with a Negative allosteric modulator (NAM) bound to it enacting conformational change. Bound ligands to a conformational changed protein may enact different effects [31].

CB2 receptors 5ZTY (Figure 4 the right-side), 6PT0 (Figure 5 left side), and 6KPC (Figure 6 left side) were selected with the similarity of CB2 bound agonists, conformation modulated receptors, and a receptor complex.Figure 7 left side displays the GPR119 complex in the GPCR family is thought to be a part of the mechanism in which cannabinoids express their effects. TRPV2 was chosen as a target as well for screening due to the implication in cancer shown in Figure 7 on the right side.

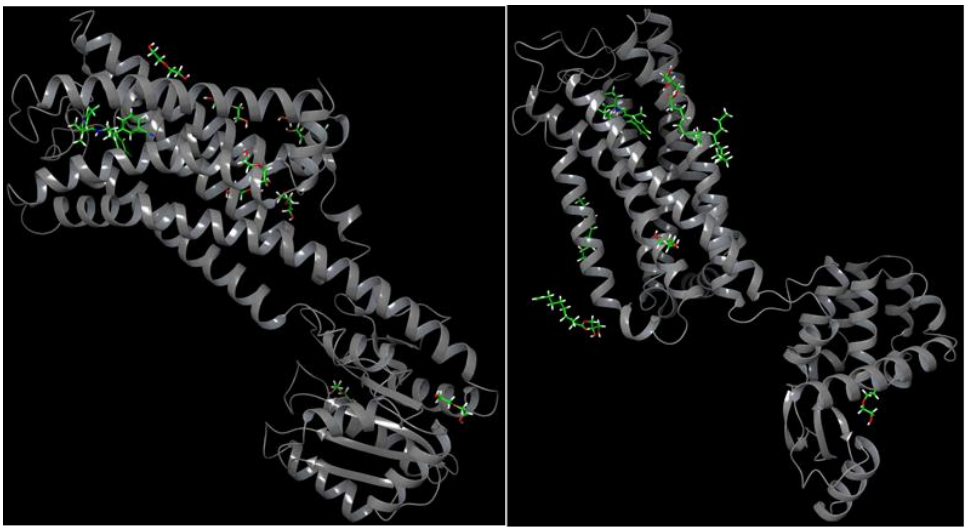

Figure 4: The protein on the left is 5U09 (crystal structure of CB1 Receptor bound to antagonist Rimonabant). The protein on the right is 5ZTY (CB2 receptor bound with an antagonist AM10257).

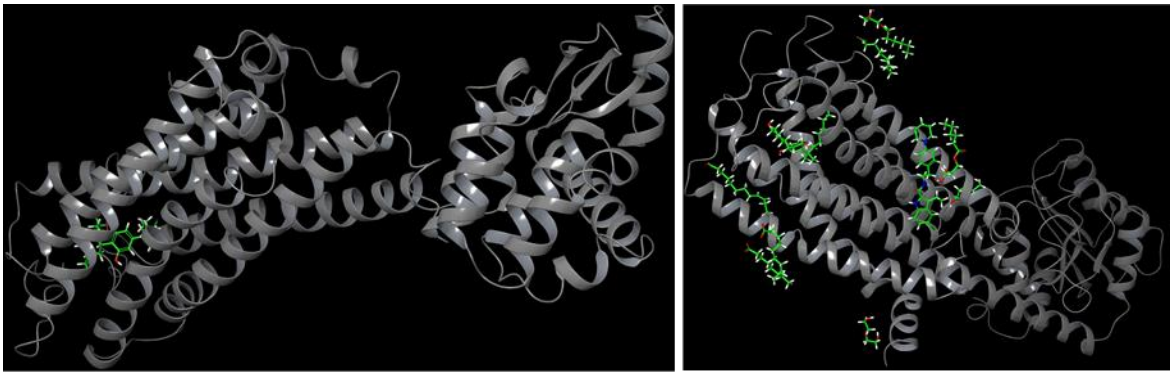

Figure 5: The protein on the left is 6KPC (CB1-CB2-Gi complex with CB2 bound agonist E3R). The protein on the right is 6KQI (CB1 receptor with an agonist CP55940).

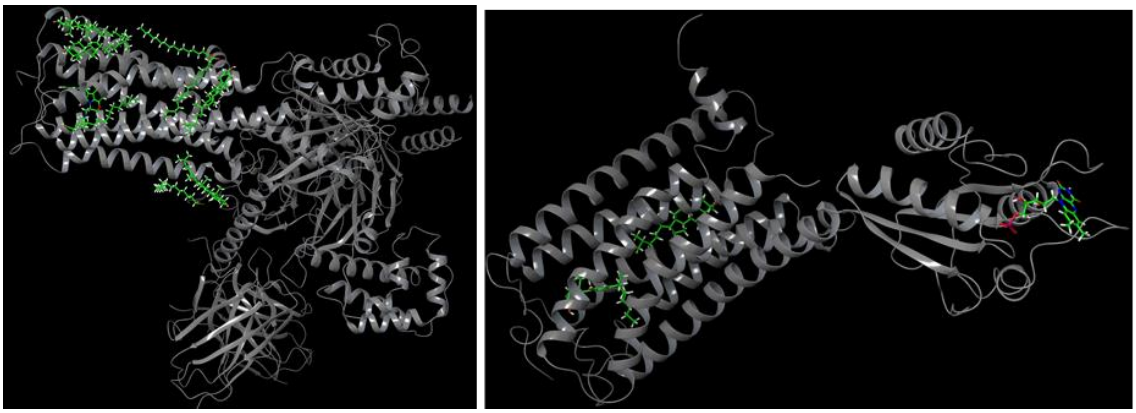

Figure 6: The protein on the left is 6PT0 (CB2-Gi signaling complex bound with an agonist WIN 55,212-2). The protein on the right is 7V3Z (CB1 receptor with a negative allosteric modulator ORG27569 bound).

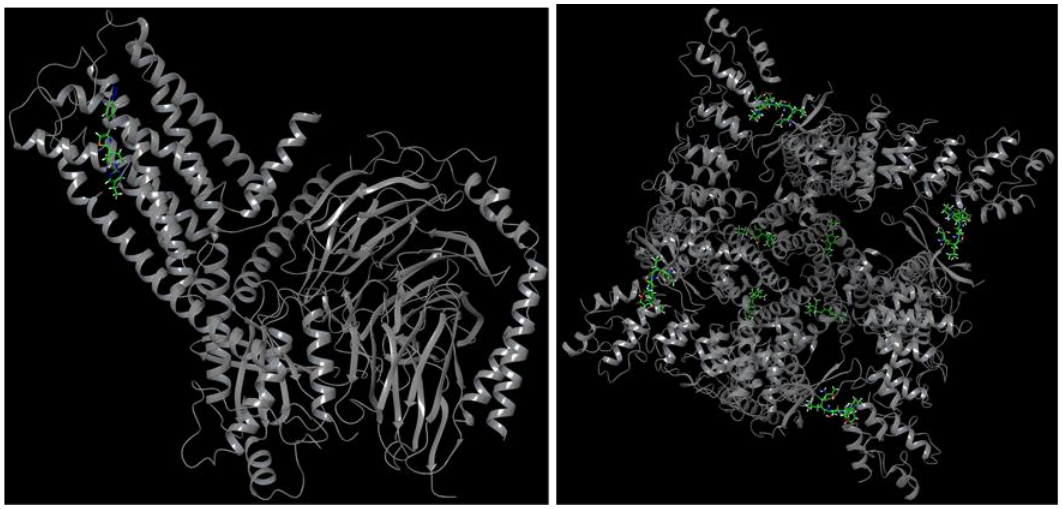

Figure 7: The protein on the left is 7WCM (GPR119-Gs complex with small molecule agonist MBX-2982 bound). The protein on the right is 8SLX (Rat TRPV2 channel with agonist CBD bound in nanodiscs).

The compounds that were bound within the receptors exhibited primarily Cation- π stacking, π-π stacking, and H-bonding. The interactions that were seen are highly important biological connections that strengthen ligand binding energies within the receptors. As displayed below in Figure 8, the cation- π interaction is shown to increase binding energy by ~2.6 kcal/mol [32], and π-π stacking additionally is seen to contribute to ligand stability within the receptor binding pocket [33]. Some of the π -stacking conformations include sandwich, T-shaped, and parallel displaced, due to the ligand conformation. H-bonding was also seen, with the solvent effect, and interaction with various water molecules, amino acid residues, and intercalation of water molecules to amino acids, the bonding kcal can vary from 1-40 kcal/mol.

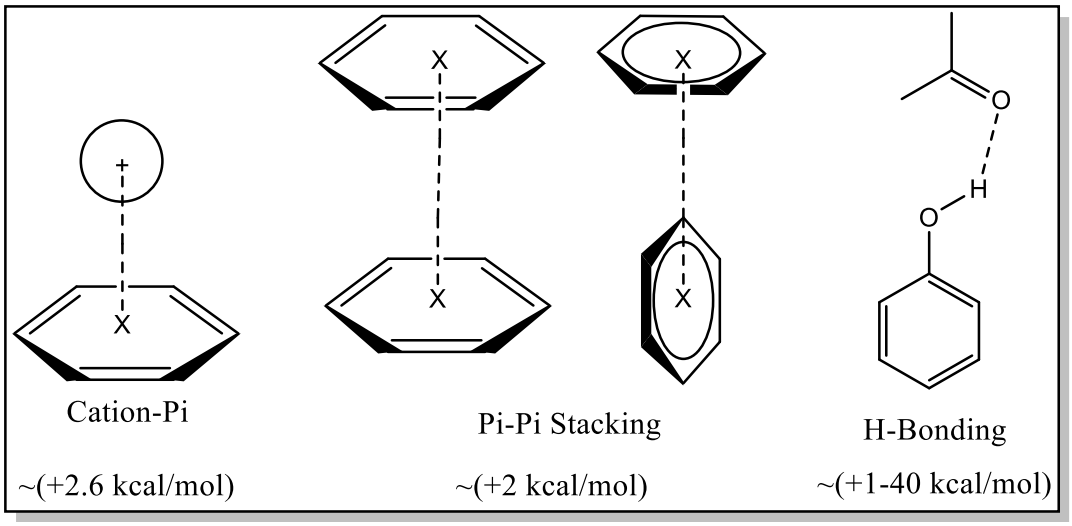

Figure 8: Common interactions found within cannabinoid receptor binding. Values are estimates based off conformation and amino acid interactions [35].

Cannabinoid agonists that activate the cannabinoid receptors (CBR) initiate pathways that can lead to inhibition or activation ultimately leading to the blocking of cell cycle, proliferation, cell death, angiogenesis, metastases, and cellular transition. Derived proteins as mentioned were

pulled from the activated/deactivated pathways which have a correlation to disease genesis or progression (Figure 9). [34,35]

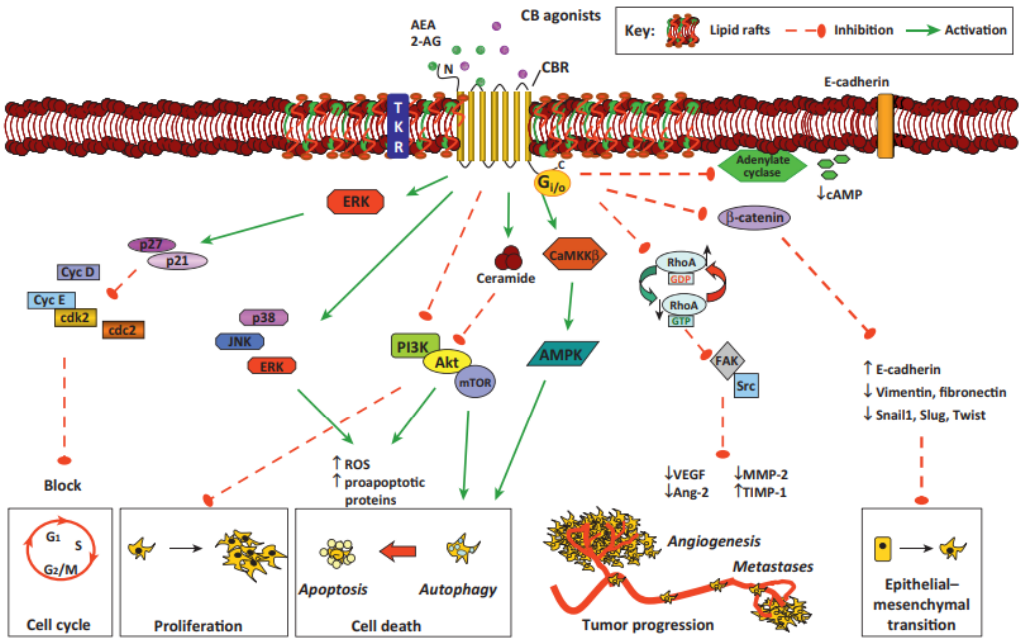

Figure 9: Cannabinoid signaling pathway [34]

In some cancer cell lines, CBD acts as a NAM of receptors CB1 and CB2; and not only blocks the cell cycle but also intensifies the ataxia protein and p53 expression levels. In addition, CBD decreases p21, CDK2, and Cyclin E protein levels (Figure 10, [36]). THC has shown to trigger cancer cell death via activation of the CB2 receptor, decrease of Cdc2, and production of ROS synthesis (Figure 10, [36]). The autophagy mechanism is induced by a combination of THC-CBD which activates the LC3-II levels or mediates the activation of TRIB3 or CaCMKKβ followed by the inactivation of mTORC2 or mTORC1 respectively (Figure 10, [36]).

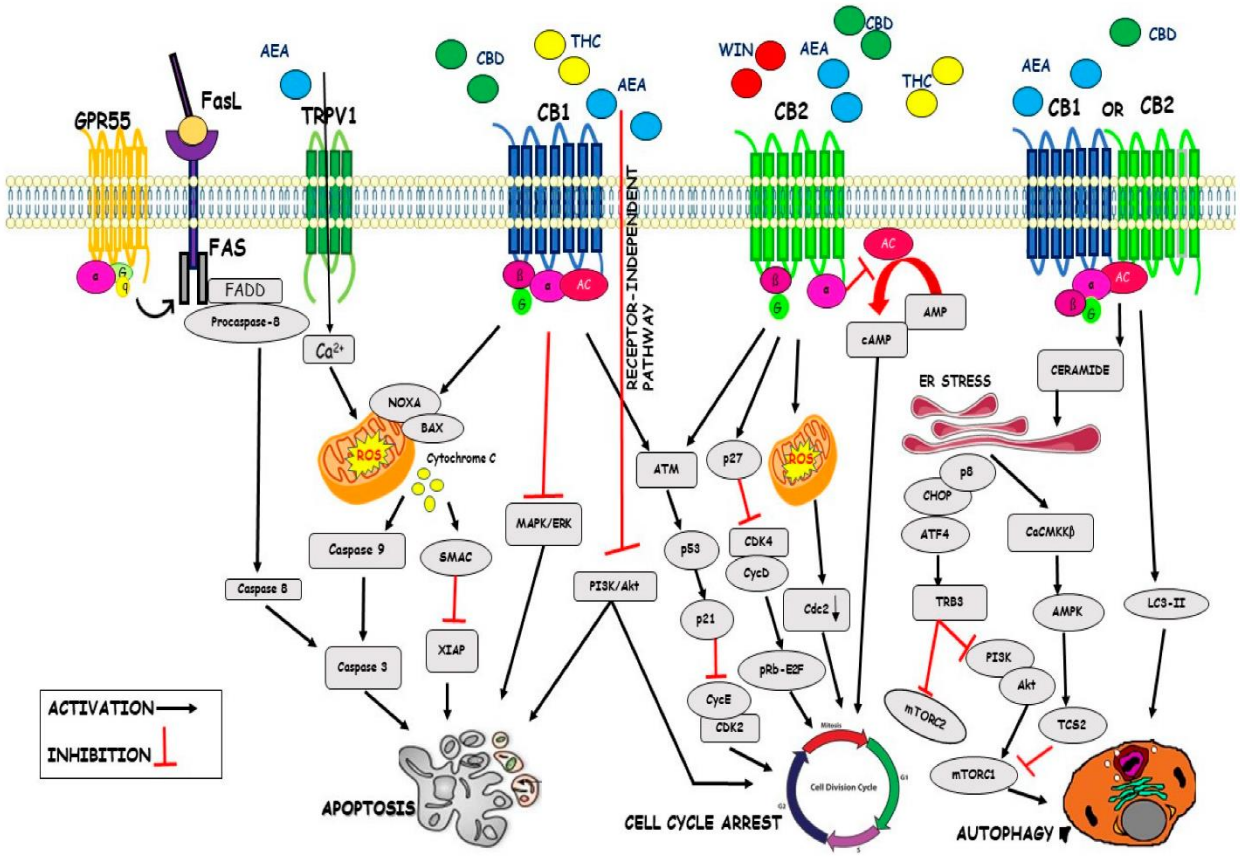

Figure 10: CBD and THC effects on signaling pathway of cell cycle, apoptosis, and autophagy [34].

2. Methods

2.1 Proteins and Ligands Preparation

All Molecular docking experiments were achieved on CybertronPC CLX 13th Gen Intel(R) Core(TM) i9-13900KF @ 3.00 GHz comprising 24 computing cores. Schrödinger Release 2023-3: Glide software was used as the docking program [31]. Crystal structures of CB_1, CB_2, GPR119, TRPV1, PAK1, and PPAR-γ were retrieved from the RCSB Protein Data Bank. CB_1 [(PDB: 7V3Z), (PDB: 5U09), (PDB: 6KQI)]. CB_2 [(PDB: 5ZTY), (PDB:6PT0), (PDB: 6KPC)]. GPR119 [(PDB: 7WCM)]. TRPV1 [(PDB: 8SLX)]. PAK1 [(PDB: 5DFP)]. PPAR-γ [(PDB: 2P4Y)].

The proteins were prepared using a protein preparation workflow tool on Schrödinger Protein Preparation Wizard [31]. The external water molecules and ions were removed. Polar Hydrogens were added. Missing side chains were filled using Epic and PROPKA. Het states were generated at pH 7.4 (+/- 2.0). Heavy atoms converged to RMSD 0.30Å. 3D structures of cannabinoids and hydrogenated cannabinoids were established in 2D sketcher which was then exported as a SDF file and imported and prepared using LigPrep, to form 3D conformers, including the various 3D chiral conformations. All structures underwent geometrical optimization using Release 2023-3: Jaguar software using density functional theory (DFT) calculation with B3LYP/6-31G as the basis set for the calculation to afford the minimized energy chemical structures. The structures were then docked using Release 2023-3: Glide software from Schrödinger.

2.2 In Silico Molecular Docking

The grid parameter was generated covering the **CB_1** pockets for (PDB:7V3Z) [-42.91, -163.58, 306.7], (PDB:5U09) [126.7,118.85,147.7], (PDB:6KQI) [-25.98, -8.77, 40.11] for x,y,z coordinates. The ligand diameter midpoint box follows a 10Å x 10Å x 10Å x,y,z dimension. The grid parameter was generated covering the **CB_2** pockets for (PDB:5ZTY) [9.09, -0.17, -55.72], (PDB:6PT0) [98.38, 109.56, 123.8], (PDB:6KPC) [10.52, 1.26, -45.17] for x,y,z coordinates. The Ligand diameter midpoint box follows a 10Å x 10Å x 10Å x,y,z dimension. The grid parameter was generated covering the **TRPV1** pocket (PDB:8SLX) [111.36, 131.77, 133.37] for x,y,z coordinates. The ligand diameter midpoint box follows a 10Å x 10Å x 10Å x,y,z dimension. The grid parameter was generated covering the **GPR119** pocket (PDB:7WCM) [126.7, 118.85, 147.7] for x,y,z coordinates. The ligand diameter midpoint box follows a 10Å x 10Å x 10Å x,y,z dimension. The grid parameter was generated covering the **PAK1** pocket (PDB:5DFP) [13.58, 34.37, -15.61] for x,y,z coordinates. The ligand diameter midpoint box follows a 10Å x 10Å x

10Å x,y,z dimension. The grid parameter was generated covering the **PPAR-γ** pocket (PDB:2P4Y) *[35.4, -21.89, 39.56_B] for x,y,z coordinates. The ligand diameter midpoint box follows a 10Å x 10Å x 10Å x,y,z dimension.

2.3. *Molecular Dynamics Simulations*

Molecular mechanics with generalized born and surface area solvation (MM-GBSA) using Release 2023-3: Prime software from Schrödinger. The minimized energy structures were received using Jaguar software, density functional theory (DFT) calculation with B3LYP/6-31G as the basis set for the calculation, and prepared proteins using the protein preparation workflow tool on the Maestro 12.5 interface of Schrödinger Protein Preparation Wizard [31]. Prime MM–GBSA (MMGBSA dG Bind (NS) and MMGBSA dG Bind) energy was calculated and displayed in Table 4-SI. MM/GBSA calculations were accomplished to esteem the relative binding energies of cannabinoids to the receptors. PDB: 8SLX could not undergo minimization and MM-GBSA due to the tetrameric crystal structure of the protein. Schrodinger has a limit of restable type residues of 500, with the protein far exceeding the limit.

2.4. Prediction of ADMET Properties

The absorption, distribution, metabolism, excretion, and toxicity (ADMET) properties of the 44 cannabinoids were performed using QikProp version 4.4 integrated into Maestro (Schrö dinger, LLC, New York, 2015) which predicts the widest variety of pharmaceutically relevant properties: QPlogS (predicted aqueous solubility), QPlogHERG (Predicted IC_{50} value for blockage of HERG K+ channels), QPPCaco (predicted apparent Caco-2 cell permeability. Caco2 cells are a model for the gut-blood barrier), QPlogBB (predicted brain/blood partition coefficient), and % Human Oral Absorption (Predicted human oral absorption in gastrointestinal tract on 0 to 100% scale). The calculated physicochemical descriptors are displayed in Table 4-

SI. QikProp bases its predictions on the full 3D molecular structure and the global minimum energy conformer of each compound was used as input for ADMET properties.

2.5. Hypothesized P450 sites of metabolism

Schrodinger P450 site of metabolism software was used to perform calculations. CYP isoform-(intrinsic reactivity) function was used to determine possible sites of metabolism (SOM).

3. Results and Discussion

3.1. Molecular Docking of Cannabinoids

We used a virtual screen of 44 identified natural and synthetic cannabinoids and their diastereomers to explore the binding interaction between cannabinoids and PPAR-γ (2P4Y), PAK1 (5DFP), CB1 receptors (5U09, 6KQI, and 7V3Z), CB2 receptors (5ZTY, 6PT0, and 6KPC), GPR119 complex (7WCM), and TRPV2 (8SLX). We selected the cannabinoids to be docked considering three main structural components: the aliphatic side chain (C1-C7 and adamantyl) at the meta-position of the phenol in the aromatic ring, saturated or not saturated ring of the terpene moiety, and monocyclic, bicyclic, or tricyclic cannabinoids. The compounds that were screened included CBD, THC, CBC, CBG, and CBN with different substituents in the side chain and their hydrogenated analogs: H_4CBD, HHC, THCBC, and THCBG (Figure 11-14). Using Jaguar to perform minimizations and calculate DFT for given scaffolds, the then minimized scaffolds were docked within the various proteins that were prepared using the Schrödinger protein preparation workflow. The relative binding energy of all docked cannabinoids was calculated to classify the intensity of protein-ligand interactions (Table 4-SI).

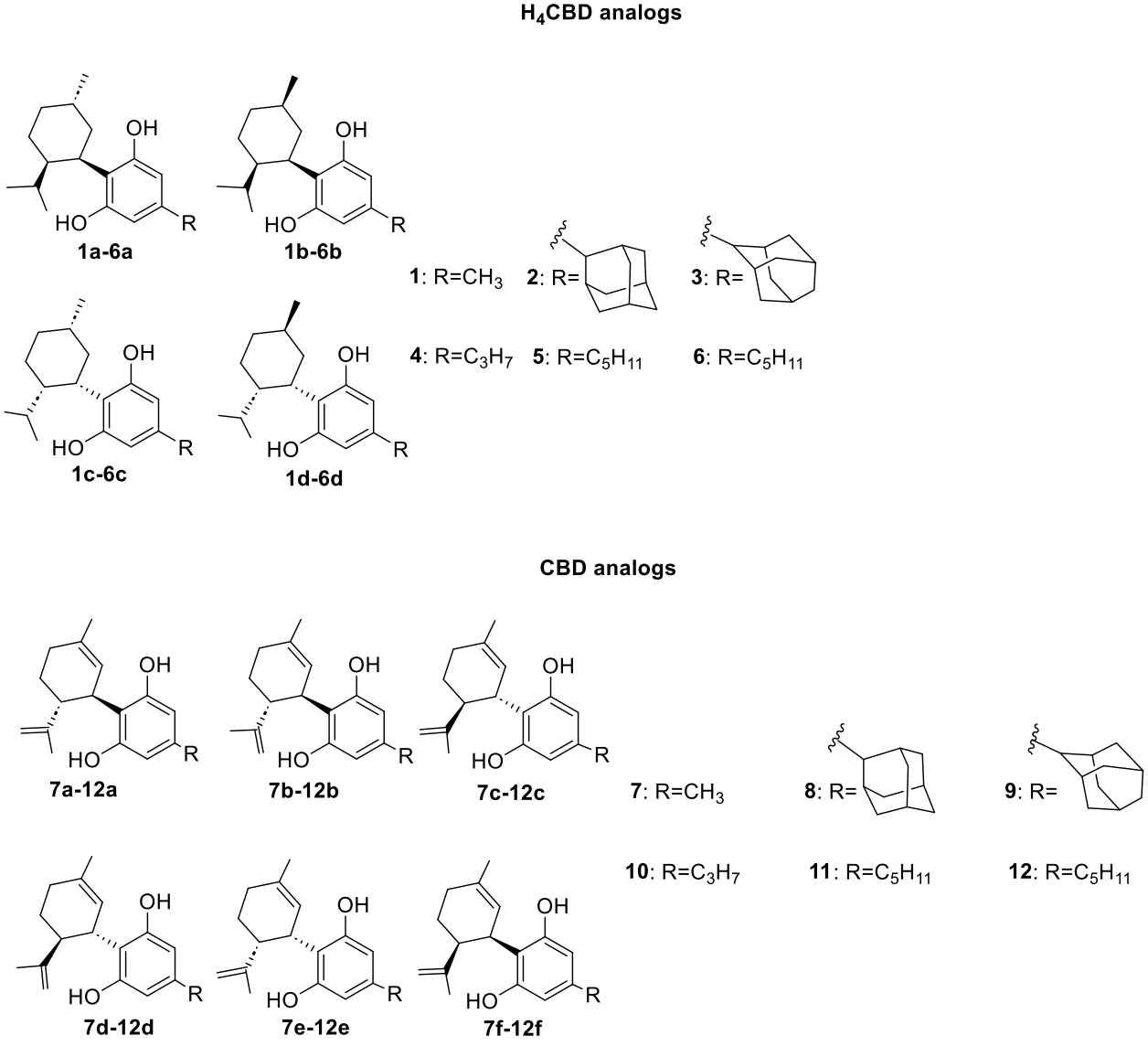

228

229 **Figure 11:** H4CBD and CBD derivatives comprising their diastereomers that were screened.

230

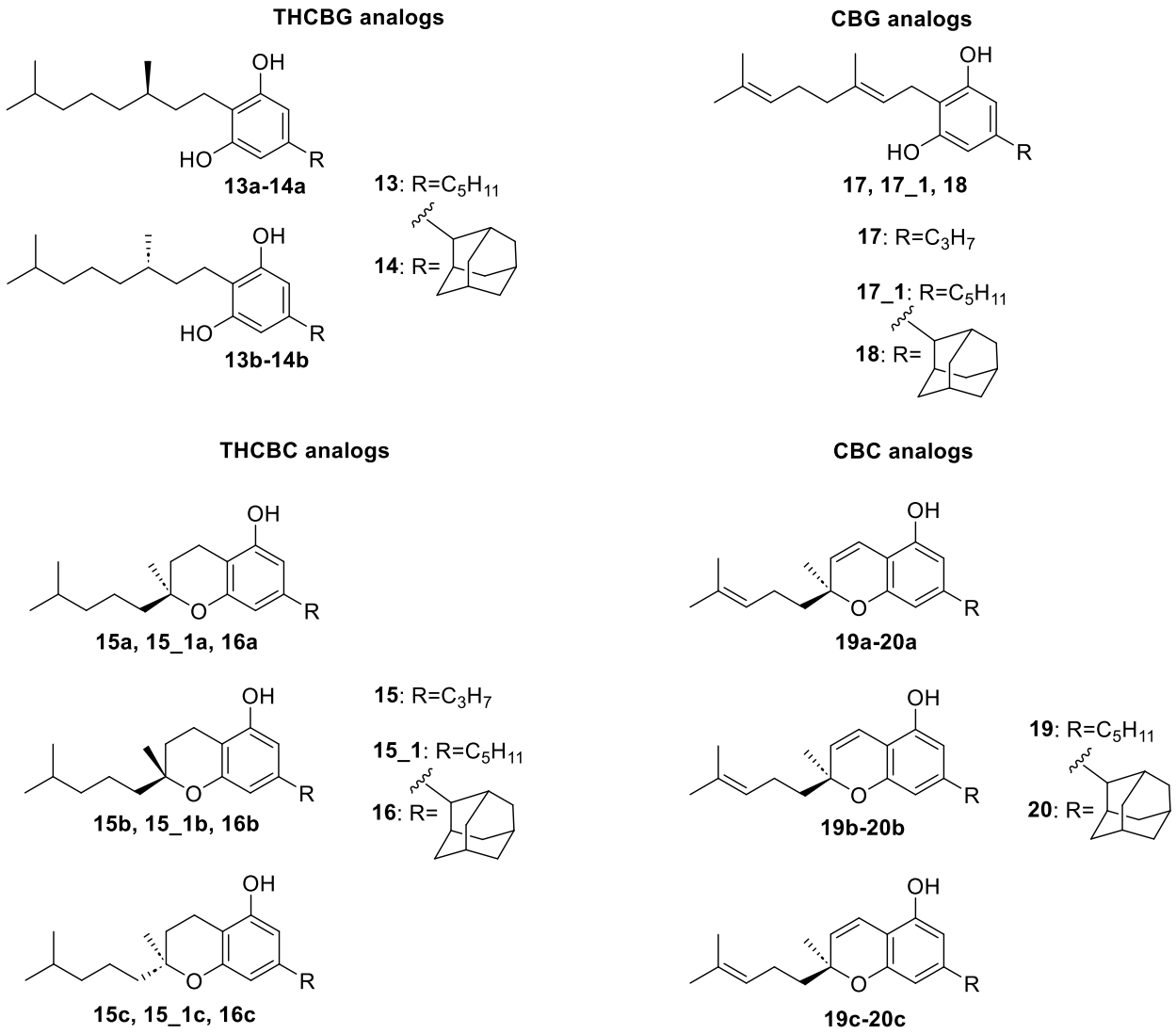

231

232 **Figure 12: T**HCBC, THCBG, CBC, and CBG derivatives comprising their diastereomers that were screened.

233

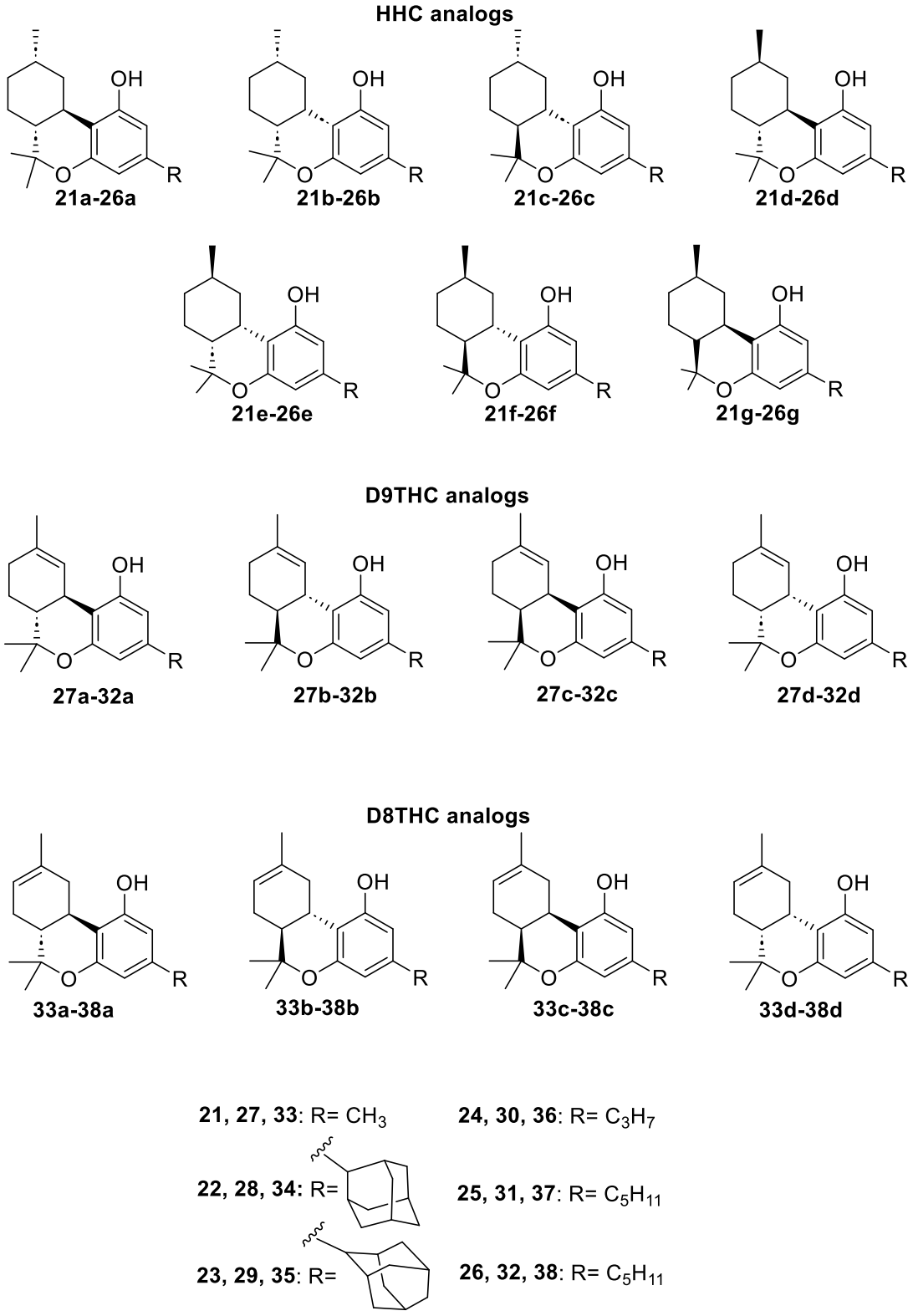

234

235 **Figure 13:** HHC, D^9THC, and D^8THC derivatives comprising their diastereomers that were screened.

236

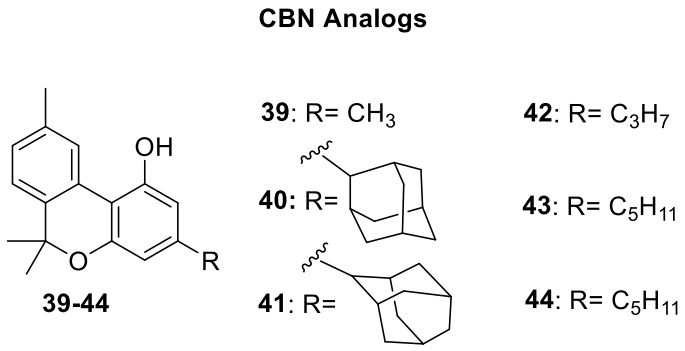

Figure 14: CBN derivatives that were screened.

The docking results showed that compounds **3**, **9**, **12**, **29**, **32**, **34**, **35**, **38**, **40-43** were not successfully docked into the CB1, CB2, GPR119, TRPV1, PAK1, and PPAR-γ models. The most favorable pose for each cannabinoid was chosen and analyzed. The docking scores ranged from -3.031 to -10.949. The docking scores of the cannabinoids are recorded in Table 3-SI. Compound **17_1** presented the most promising docking score of -10.949 with 6KPC protein (CB2 receptor), and compound **8** showed the least promising docking score of -3.031 with 5DFP (PAK1 receptor). The relative binding energies were determined by the Prime MM-GBSA module and extended from -86.054 kcal/mol (**16:7V3Z** complex) to -7.915 kcal/mol (**15_1:5U09** complex) for cannabinoids (Table 4-SI).

Next, Table 1 shows the cannabinoids that were coupled, which are colored with the type of interaction associated with the corresponding color. The common motifs of the docked cannabinoids were π-Cation, H-bonding, and π-π stacking. All the residues were within 4Å of the interacting moiety.

Protein interaction characteristics: 2P4Y, 5DFP, 5U09, 5ZTY, 6KPC, 6KQI, 6PT0, 7V3Z, 7WCM, 8SLX		
Cannabinoid	Protein (PDB)	Interaction Type
1a	5DFP, 5U09, 5ZTY, 6KPC, 6KQI, 8SLX	π-Cation, π-π stacking, π-π stacking, H-bonding
1b	5DFP, 5U09, 5ZTY, 6KQI	π-Cation, H-bonding, π-π stacking, π-π stacking
1d	6PT0, 7V3Z	H-bonding, π-π stacking
2a	6PT0	H-bonding, π-π stacking, π-π stacking

2b	2P4Y, 5ZTY, 6KPC, 6KQI	π-π stacking, π-π stacking, H-bonding
2c	6KPC, 6PT0	π-π stacking, H-bonding, H-bonding
2d	2P4Y, 6KPC	π-Cation, π-π stacking, H-bonding
3	No Docking affinity	No interaction Type
4a	2P4Y, 5ZTY, 6KQI, 6PT0	H-bonding, H-bonding
4b	5U09, 6KQI, 6PT0, 7WCM	π-π stacking, H-bonding
4c	5DFP, 7V3Z	π-Cation, π-π stacking, H-bonding
4d	5DFP, 6KPC	π-Cation, H-bonding, π-π stacking, H-bonding
5b	5DFP, 5U09	π-Cation
5c	5ZTY, 6KPC, 8SLX	π-π stacking, π-π stacking, H-bonding
6	5ZTY, 7V3Z, 8SLX	π-π stacking,H-bonding,π-π stacking,H-bonding
6b	5ZTY, 7V3Z, 8SLX	π-π stacking, π-π stacking, H-bonding, H-bonding
7a	2P4Y, 5U09, 5ZTY, 6KPC, 6PT0, 8SLX	π-Cation, π-π stacking, π-π stacking, H-bonding, H-bonding, π-π stacking
7b	5DFP, 5U09, 6KPC, 6KQI, 6PT0, 7V3Z, 7WCM	π-π stacking, π-π stacking, H-bonding, π-π stacking, π-π stacking, H-bonding
7c	2P4Y, 5DFP	H-bonding, H-bonding
8c	5DFP, 7V3Z	π-π stacking, H-bonding
8d	6KPC, 6PT0	π-π stacking, H-bonding, π-π stacking
9	No Docking affinity	No interaction Type
10a	2P4Y, 5DFP, 5U09, 5ZTY, 6KQI, 6PT0	π-Cation, π-Cation, π-π stacking, H-bonding, π-π stacking
10b	5U09, 5ZTY, 6KPC, 6KQI, 6PT0	π-π stacking, H-bonding, π-π stacking, π-π stacking
10c	2P4Y, 5DFP, 7V3Z	π-Cation, H-bonding, π-π stacking, H-bonding
10d	6PT0	H-bonding
10e	2P4Y, 5U09, 6PT0, 7V3Z	π-π stacking, H-bonding, π-π stacking, H-bonding
10f	6KPC, 6KQI	π-π stacking, π-π stacking
11a	2P4Y, 5DFP, 5U09, 6KPC, 6KQI	π-Cation, π-Cation, H-bonding
11b	2P4Y, 5U09, 5ZTY, 6KPC, 6KQI	π-π stacking, π-π stacking, π-π stacking
11c	6PT0, 7V3Z	π-π stacking, H-bonding
11d	6PT0	
11e	6KQI	
11f	2P4Y, 5U09, 6KPC	π-Cation, H-bonding, π-π stacking, H-bonding
12	No Docking affinity	No interaction Type
13a	5DFP, 5U09, 5ZTY, 6KQI, 6PT0, 7V3Z	π-Cation, π-π stacking, π-π stacking, H-bonding, π-π stacking, H-bonding
13b	6KPC, 8SLX	π-π stacking, H-bonding, π-π stacking

14a	6KQI, 6PT0, 7V3Z, 7WCM	π-π stacking
14b	5ZTY, 6KPC	π-π stacking, H-bonding
15a	2P4Y, 5DFP, 5U09, 5ZTY, 6KPC, 6PT0, 7V3Z, 7WCM	H-bonding, π-π stacking, π-π stacking, H-bonding, π-π stacking
15_1a	5DFP, 5U09, 5ZTY, 6KPC, 6KQI, 6PT0, 7V3Z, 7WCM	H-bonding, π-π stacking, π-π stacking, π-π stacking, π-π stacking, H-bonding, π-π stacking, H-bonding
16a	2P4Y, 5DFP, 6KPC, 6KQI, 6PT0, 7V3Z	π-π stacking, π-π stacking, π-π stacking, H-bonding
17	2P4Y, 5DFP, 5U09, 5ZTY, 6KPC, 6KQI, 6PT0, 7V3Z, 7WCM	H-bonding, H-bonding, π-π stacking, H-bonding, π-π stacking, H-bonding, π-π stacking, π-π stacking, H-bonding
17_1	2P4Y, 5DFP, 5U09, 5ZTY, 6KPC, 6KQI, 6PT0, 7V3Z, 7WCM, 8SLX	H-bonding, H-bonding, H-bonding, π-π stacking, H-bonding, π-π stacking, H-bonding, π-π stacking, H-bonding, π-π stacking, H-bonding, π-π stacking, H-bonding, π-π stacking, H-bonding, H-bonding
18	5ZTY, 6KPC, 6KQI, 6PT0	π-π stacking, π-π stacking, H-bonding, π-π stacking, π-π stacking
19a	2P4Y, 5DFP, 5U09, 5ZTY, 6KPC, 6KQI, 7V3Z, 7WCM, 8SLX	π-Cation, H-bonding, π-π stacking, π-π stacking, π-π stacking, H-bonding, π-π stacking, H-bonding
20a	5DFP, 5ZTY, 6KQI, 6PT0, 7V3Z	H-bonding, π-π stacking, π-π stacking
21a	2P4Y, 5DFP, 5ZTY, 6KQI, 6PT0	H-bonding, H-bonding, H-bonding, π-π stacking
21b	2P4Y, 5U09, 5ZTY, 6KPC, 6KQI, 6PT0, 7WCM	H-bonding, π-π stacking, π-π stacking, π-π stacking
21c	2P4Y, 5DFP, 5ZTY, 6KPC, 6KQI, 6PT0, 7V3Z, 7WCM	π-Cation, H-bonding, H-bonding, π-π stacking, π-π stacking, H-bonding, H-bonding, π-π stacking, H-bonding, π-π stacking, H-bonding
21d	2P4Y, 5DFP, 5U09, 6KPC, 6PT0, 8SLX	π-Cation, H-bonding, H-bonding, π-π stacking
21e	2P4Y, 5DFP, 5U09, 5ZTY, 6KPC, 6KQI, 6PT0, 7WCM	π-Cation, H-bonding, H-bonding, π-π stacking, π-π stacking, π-π stacking, H-bonding, π-π stacking, π-π stacking, H-bonding
21f	5ZTY	π-π stacking
22c	5ZTY, 6KPC, 6KQI, 6PT0, 7V3Z	π-π stacking, π-π stacking, H-bonding, π-π stacking, π-π stacking, H-bonding
23c	5ZTY, 6PT0	π-π stacking
23d	7V3Z	π-π stacking, H-bonding
24a	2P4Y, 5U09, 5ZTY, 6KPC, 6KQI, 6PT0	H-bonding, π-π stacking, π-π stacking, π-π stacking, π-π stacking

24b	2P4Y, 5U09, 5ZTY, 6KPC, 6PT0, 7WCM	π-π stacking, H-bonding, H-bonding, π-π stacking
24c	5ZTY	π-π stacking
24d	2P4Y, 5DFP, 5U09, 5ZTY, 6KPC, 6PT0	H-bonding, π-π stacking, H-bonding, π-π stacking
24e	2P4Y, 5DFP, 5U09, 5ZTY, 6PT0, 7WCM	π-Cation, H-bonding, π-π stacking, π-π stacking, H-bonding
24f	2P4Y, 5DFP, 6KPC, 7WCM	π-Cation, H-bonding, H-bonding, H-bonding, π-π stacking, H-bonding
24g	5DFP, 5U09, 5ZTY, 6KPC, 6KQI, 6PT0, 7WCM	π-Cation, π-π stacking, π-π stacking, π-π stacking, π-π stacking, π-π stacking, H-bonding
25c	2P4Y, 5U09, 6KPC, 6KQI, 7V3Z, 7WCM	π-Cation, H-Bonding, π-π stacking, H-bonding, π-π stacking, π-π stacking, H-bonding
25f	2P4Y, 5U09, 6KPC, 6KQI, 6PT0, 8SLX	π-Cation, H-bonding, π-π stacking, π-π stacking, π-π stacking
25g	2P4Y, 5DFP, 5ZTY, 6KQI, 6PT0	π-Cation, H-bonding, π-π stacking, π-π stacking
26c	2P4Y, 5U09, 5ZTY, 6KPC, 6KQI, 6PT0, 7V3Z, 7WCM	π-Cation, H-bonding, π-π stacking, π-π stacking, π-π stacking, H-bonding, H-bonding, π-π stacking, H-bonding, π-π stacking, H-bonding
27a	2P4Y, 5DFP, 5U09, 5ZTY, 6KPC, 6KQI, 6PT0, 7WCM	H-bonding, π-π stacking, H-bonding, π-π stacking, π-π stacking
27b	2P4Y, 5DFP, 5U09, 5ZTY, 6KPC, 6KQI, 6PT0, 7V3Z	H-bonding, π-π stacking, π-π stacking, π-π stacking, π-π stacking, H-bonding
27c	2P4Y, 6KPC, 6KQI, 6PT0	H-bonding, π-π stacking, π-π stacking, H-bonding, π-π stacking
27d	5DFP, 5U09, 5ZTY	π-π stacking
28b	5DFP, 5ZTY, 6KPC, 6KQI, 6PT0	π-π stacking, H-bonding, π-π stacking
29	No Docking affinity	No interaction Type
30a	2P4Y, 5DFP, 5U09, 5ZTY, 6KPC, 6KQI, 6PT0, 7V3Z	π-Cation, π-π stacking, H-bonding, π-π stacking
30b	5DFP, 5U09, 5ZTY, 6KPC, 6KQI, 6PT0, 7V3Z, 8SLX	H-bonding, π-π stacking, π-π stacking, π-π stacking, π-π stacking, π-π stacking
31b	2P4Y, 5DFP, 5U09, 5ZTY, 6KPC, 6KQI, 6PT0, 7V3Z	π-Cation, H-bonding, H-Bonding, H-bonding, π-π stacking, π-π stacking, H-bonding, π-π stacking, H-bonding
31c	2P4Y, 5U09, 5ZTY, 6KPC, 6KQI, 6PT0, 7WCM	π-Cation, H-bonding, π-π stacking, π-π stacking, H-bonding, π-π stacking
31d	2P4Y, 5DFP, 5U09, 5ZTY, 6KQI, 6PT0, 7V3Z	H-Bonding, π-π stacking, π-π stacking, H-bonding, π-π stacking
32	No Docking affinity	No interaction Type
33a	2P4Y, 5U09, 5ZTY, 6KPC, 6PT0, 7V3Z, 8SLX	π-Cation, π-π stacking, H-bonding, π-π stacking, π-π stacking, π-π stacking

33c	2P4Y, 5DFP, 5U09, 5ZTY, 6KPC, 6KQI, 6PT0, 7WCM	H-bonding, π-π stacking, π-π stacking, H-bonding, π-π stacking, π-π stacking, H-bonding, π-π stacking
33d	5DFP, 5U09, 5ZTY, 6KPC, 6KQI, 6PT0, 7WCM	H-bonding, π-π stacking, π-π stacking, π-π stacking, H-bonding
34	No Docking affinity	No interaction Type
35	No Docking affinity	No interaction Type
36b	5DFP, 5U09, 5ZTY, 6KPC, 6PT0, 7V3Z	H-bonding, π-π stacking, π-π stacking, π-π stacking, π-π stacking
36c	2P4Y, 5DFP, 5U09, 5ZTY, 6KPC, 6KQI, 6PT0, 7WCM	π-Cation, π-π stacking, H-bonding, π-π stacking, π-π stacking, H-bonding
36d	2P4Y, 5DFP, 5U09, 5ZTY, 6KPC, 6KQI, 6PT0	H-bonding, π-π stacking, H-bonding, π-π stacking, π-π stacking, π-π stacking, H-bonding
37c	2P4Y, 5DFP, 6KQI	π-Cation, π-Cation, H-bonding, π-π stacking
37d	5U09, 7V3Z	H-bonding, π-π stacking
38	No Docking affinity	No interaction Type
39	2P4Y, 5DFP, 5U09, 5ZTY, 6KPC, 6KQI, 6PT0, 7V3Z, 7WCM	π-Cation, π-π stacking, π-π stacking, π-π stacking, π-π stacking, π-π stacking, H-bonding
40	No Docking affinity	No interaction Type
41	No Docking affinity	No interaction Type
42	No Docking affinity	No interaction Type
43	No Docking affinity	No interaction Type
44	2P4Y, 5DFP, 5U09, 5ZTY, 6KPC, 6KQI, 7V3Z	π-Cation, H-bonding, π-π stacking, π-π stacking, π-π stacking, π-π stacking, π-π stacking, H-bonding

Table 1: The table represents according to color the association of the protein and type of interactions. Some of the compounds have no binding affinity information and are described. Some compounds docked with the protein but showed no interaction.

PPAR-γ (2P4Y)

Figure 1-SI and Table 2-SI show the cannabinoids and their interactions with the PPAR-γ (2P4Y) model. CBG-5C (**17_1**) was demonstrated to exhibit the greatest favorable docking score of -8.241 and CBG-3C (**17**) was proven to display the least promising docking score of -4.772 (Table 3-SI). CBG-5C (**17_1**) has H-bonding with Leu340 residue and CBG-3C (**17**) has H-bonding with H_2O. Cannabinoids (CBD-5C:**11f**, HHC-1C:**21c**, HHC-3C:**24f**) that resulted in high docking scores and relative binding energies ranged between -42.402 kcal/mol and -50.369 kcla/mol (Table 4-SI) presented multiple interactions with the 2P4Y protein: H-bond interaction

between phenolic hydroxyl groups (from resorcinol moiety) and Leu340, Cys285, and H_2O residues. Also, the resorcinol ring exhibited π-cation interaction with Arg288 residue. It is interesting to note that compound **27b** (D^9THC-1C) exhibited the strongest relative binding energy complex D^9THC-1C:2P4Y (MMGBSA dG Bind(NS)= 59.605kcal/mol: Table 4-SI) with a very good docking score (-7.553) and was the only cannabinoid that displayed H-bonding interaction with Ser289, which is the major interaction presented by the indole reference ligand (Figure 15). Brunsveld [37] proved that indazole MRL-871 interacts with PPARγ Ser289 residue via hydrogen bond and plays a key role in the stabilization of the beta-sheet region of PPARγ receptor.

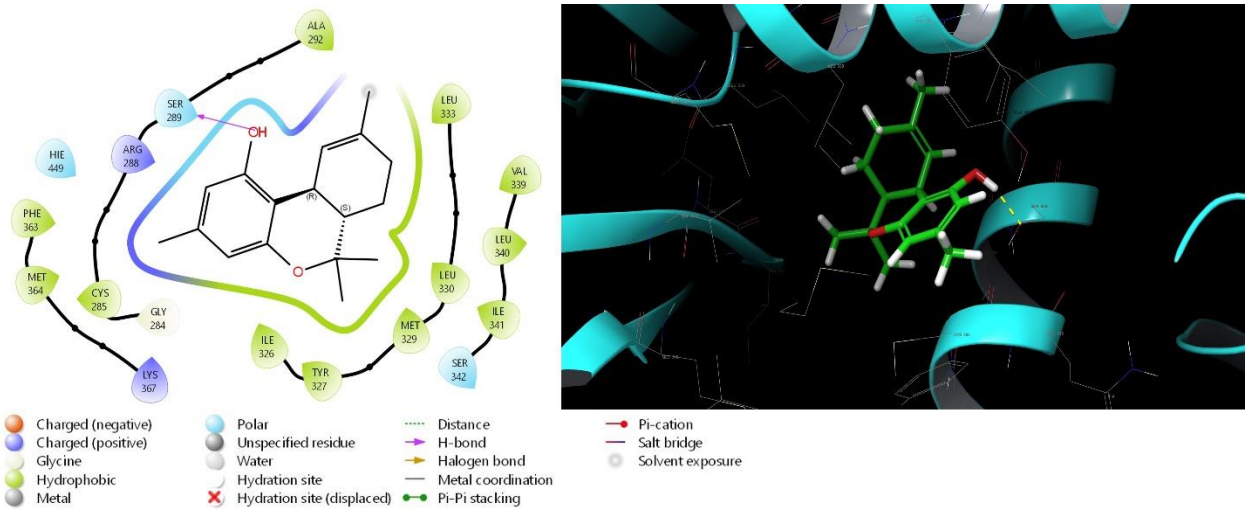

Figure 15: 3D and 2D diagrams of interactions of compound **27b** with 2P4Y where yellow dotted line represents the H-bond in the 3D diagram.

PAK1 (5DFP)

Figure 2-SI and Table 2-SI indicate the interactions of docked cannabinoids with the PAK1 (5DFP) model and the FRAX1036 as inhibitor ligand. The docking results showed that 25 cannabinoids out of 44 were successfully docked into the 5DFP protein. The highest docking score corresponds to CBN-7C (**44**) with -6.309 and the lowest is -3.031 for CBD-Adamantyl (**8**)

as shown in Table 3-SI. CBN-7C (**44)** interacted with Asp393, and H_2O forming a conventional hydrogen bond with each of these two residues. Interaction of CBN-7C (**44)** with 5DFP, both 3D and 2D diagrams are shown in Figure 16. The complex of CBN-7C (**44)** :5DFP was found to exhibit the strongest MMGBSA dG Bind (NS) energy with -57.664 kcal/mol (Table 4-SI).

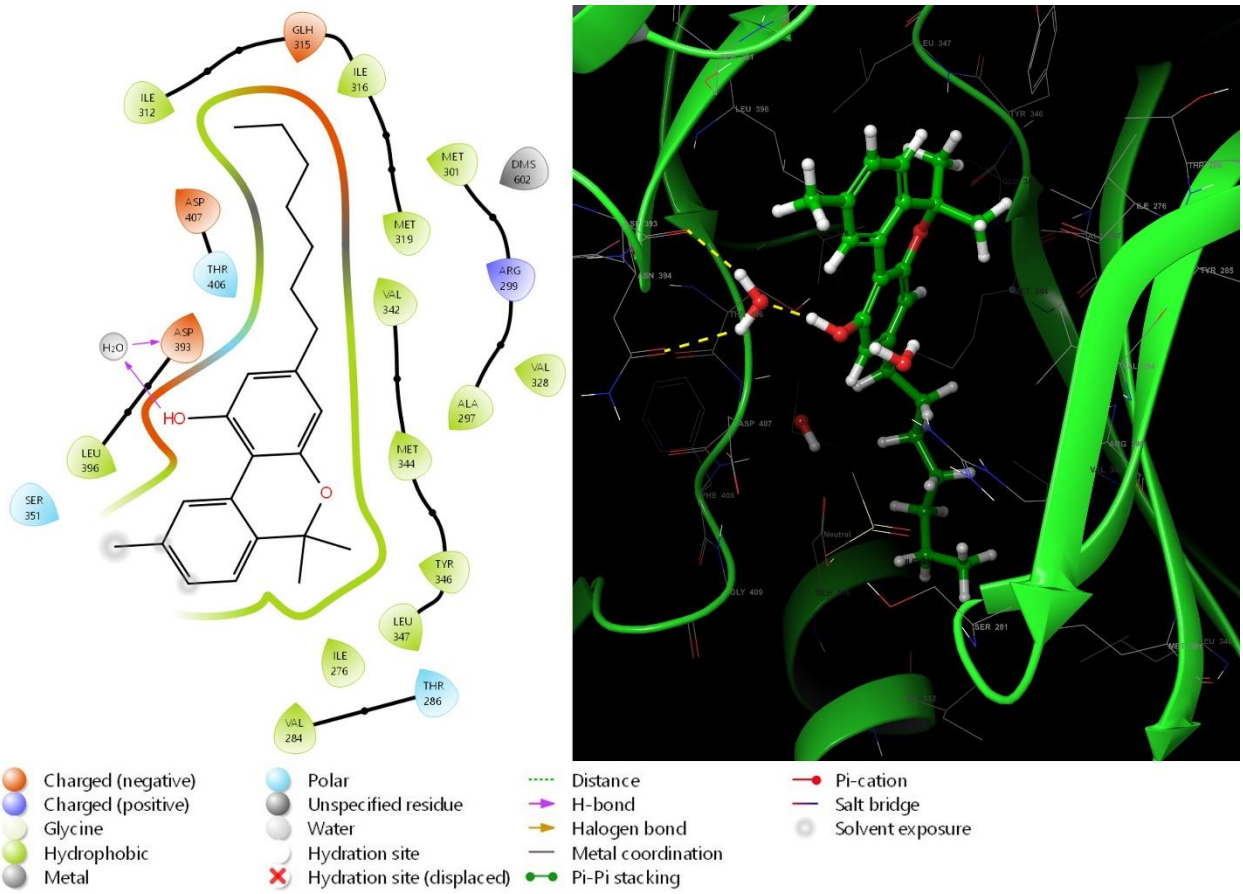

Figure 16: 3D and 2D diagrams of interactions of compound **44** with 5DFP where yellow dotted line represents the H-bond in the 3D diagram.

The frequent interaction pattern that was observed among the cannabinoids and the residues includes π-cation (Arg299 with phenyl ring from resorcinol moiety) and aromatic hydrogen bond (Thr406, Leu347, Gluc345, Gluc315, Asp393, H_2O). The interaction pattern was compared with the inhibitor FRAX1036 of the PAK1 crystal structure which showed hydrogen bond interactions with Glu 67, Gluc315, H_2O, Arg51, Leu 99, Asp 106, Asp393, and Thr406.

Compounds H_4CBD-3 (**4d**), CBD-3C (**10c**), HHC-1C (**21c**), HHC-3C (**24f**), HHC-5C (**25g**), D_8THC-3C (**36d**), and D_8THC-5C (**37c**) revealed two interactions with the amino acid residues showing -5.333, -5.288, -5.249, -5.909, -5.162, -5.846, and -5.604 as docking scores, respectively (Table 3-SI). Prime MM-GBSA analysis disclosed the relative binding energies of these cannabinoids to 5DFP as -45.361 kcal/mol, -45.093 kcal/mol, -46.470 kcal/mol, -44.633 kcal/mol, -47.970 kcal/mol, -40.275 kcal/mol, and -48.539 kcal/mol, correspondingly (Table 4-SI).

Nikfarjam [38] demonstrated that CBD and THC inhibited pancreatic cancer progression moderately through inhibition of PAK1. Considering this preliminary *in silico* study of different cannabinoids we suggest that compounds H_4CBD-3C (**4d**), CBD-3C (**10c**), HHC-1C (**21c**), HHC-3C (**24f**), HHC-5C (**25g**), D_8THC-3C (**36d**), and D_8THC-5C (**37c**) and CBN-7C (**44**) could be good inhibitors of PAK1 and therefore could be used in the treatment of pancreatic cancer.

CB1 (5U09, 6KQI, 7V3Z) and CB2 (5ZTY, 6KPC, 6PT0,)

Since CB1 and CB2 receptors have been discovered as meaningful molecule targets for some common disorders, the identification and design of new modulators for CB1 and CB2 are crucial. The *in-silico* study of the interactions of cannabinoids with CB1 and CB2 receptors occupies a prominent place in the discussion of the agonist, antagonist, and positive or negative allosteric modulator activity of these ligands on the receptors.

Allosteric ligands have been studied in the last 20 years because they present better receptor selectivity and potency than orthosteric ligands due to allosteric positions are less preserved across proteins and the opposition with endogenous is eliminated [39-41]. Allosteric modulators can be positive allosteric modulators (PAM) or NAM [42]. A PAM improves the affinity,

potency, and/or efficacy of the ligand whereas a NAM decreases the affinity, potency, and/or efficacy of the ligand [43].

In this work, we selected Rimonabant and AM10257 as antagonist ligands of 5U09 (CB1 receptor) and 5ZTY (CB2 receptor) respectively. CP55940, E3R, and WIN 55,212-2 as agonist ligands of 6KQI (CB1 receptor), 6KPC (CB2 receptor), and 6PT0 (CB2 receptor) respectively. ORG27569b as a negative allosteric modulator of 7V3Z (CB1 receptor).

Figure 3-8-SI and Table 2-SI show the interactions between amino acids on the protein mentioned above and functional groups on tested cannabinoids, Table 3-SI displays the docking scores, and Table 4-SI exhibits the Prime MM–GBSA energies.

For protein 5U09, which is bound to the antagonist rimonabant of CB1 receptor, the highest docking score is -10.321 corresponding to CBG-5C (**17_1**) and the lowest is -4.770 for CBG-3C (**17**) as shown in Table 3-SI. CBG-5C (**17_1**) exhibited multiple interactions type H-bond with the residues Ser383 and Met 103 via OH groups in the aromatic ring. Also showed π- π stacking interaction between aromatic ring-A and Phe268 amino acid residue (Figure 17). These residues are fragments of the deep binding pocket crucial for effective ligand binding. These interactions are similar to those shown by Rimonabant, a known CB1 receptor antagonist. In addition, the CBG-5C: 5U09 complex was found with -52.341 kcal/ mol MM–GBSA: MMGBSA dG Bind (NS) being the best relative binding energy complex (Table 4-SI).

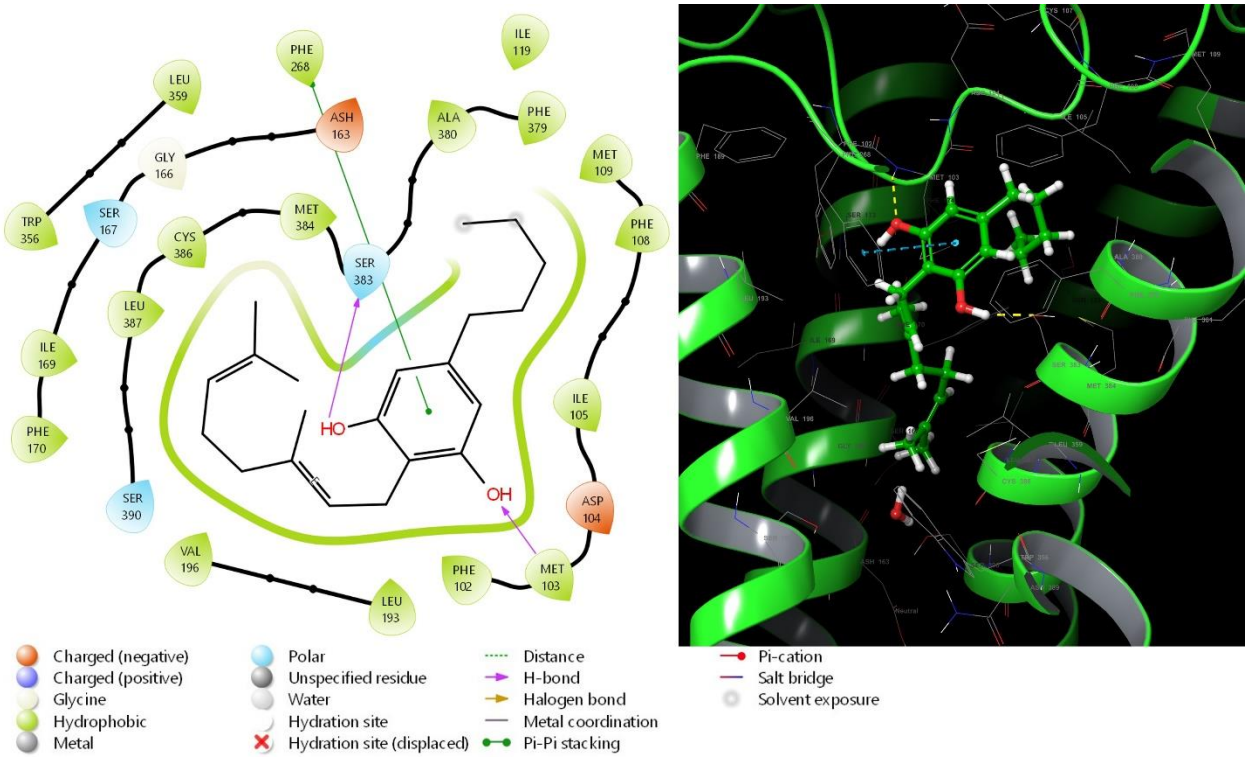

Figure 17: 3D and 2D diagrams of interactions of compound **17_1** with 5UO9 where yellow dotted lines represent the H-bond and blue dotted line represents the π- π stacking interaction in the 3D diagram.

For protein 5ZTY, which is bound with AM10257 an antagonist of the CB2 receptor, the results show that twenty-five cannabinoids of forty-four docked cannabinoids interacted with the amino acid residues of this protein (Figure 4-SI). The best docking score is -10.009 which corresponds to CBG-5C (**17_1**) and the worst is -4.770 for CBG-3C (**17**) (Table 3-SI). However, CBG-5C (**17_1**) only displayed an H-bond interaction with Leu182, which is not a key residue in the binding pocket of the CB2 receptor. The cannabinoids:5ZTY complexes that presented the stronger relative binding energies, good docking scores and multiple interaction types π- π stacking and H-bond with the residues are H_4CBD-7C (**6b**), CBD-1C (**7a**, **7b**), THCBC-5C (**15_1a**), CBC-5C (**19a**), HHC-1C (**21b**, **21c**, **21e**, **21f**), HHC-C3 (**24d**, **24g**), HHC-C5 (**25g**) D^9 THC-3C (**30a**), D^9THC (**31b**), CBN-1C (**39**), and CBN-7C (**44**). Phe87, Phe183, and Trp194 were the most relevant amino acids in the binding pocket. The residues implied in these cannabinoid bindings match those identified in the AM10257 antagonist-binding motif. The

interactions took place in the resorcinol moiety and phenolic groups. Interestingly, HHC-1C (**21e**) is the only ligand that interacts via π- π stacking and H-bond as shown in the 2D and 3D diagrams in Figure 18.

These *in silico* results demonstrate that THCBC (**15_1a**), CBC (**19a**), HHCs, and D^{9}THCs have the most promising interactions with 5ZTY and could be possible antagonists of the CB2 receptor.

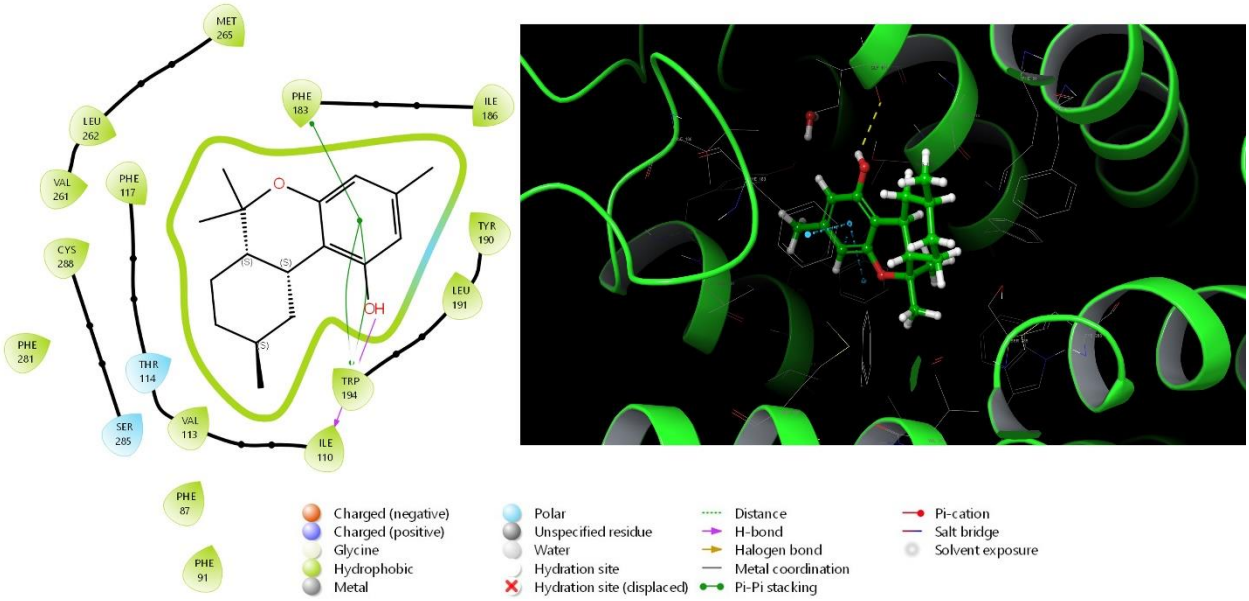

Figure 18: 3D and 2D diagrams of interactions of compound **21e** with 5ZTY where yellow dotted lines represent the H-bond and blue dotted line represents the π- π stacking interaction in the 3D diagram.

The results from our docking study with protein 6KQI with bound CP55940 ligand as an orthosteric agonist of CB1 receptor established that 30 cannabinoids successfully docked into the binding pocket of this protein (Figure 5-SI, Table 2-SI, Table 3-SI, Table 4-SI). The cannabinoids that exhibited multiple interactions with amino acid residues of 6KQI, greater binding energy for 6KQI protein, and a docking score higher than -7 were THCBG-5C (**13a**), THCBC-5C (**15_1a**), CBG-5C(**17_1**), CBC-5C (**19a**), HHC-3C (**24a**), D^{9}THC-1C (**27b**), D^{9}THC-adamantyl (**28b**) D^{9}TH-3C (**30b**), D^{9}THC-5C (**31b**, **31c**, **31d**), D^{8}THC-5C (**36c**, **36d**) and CBN-C7 (**44**). These cannabinoids interacted with Phe170, and Phe268 forming a π- π stacking bond, and

with Ser383 forming an H-bond in similar patterns to CP55940. CBC-5C (**19a**) displayed the highest docking score with -10.003 (Table 3-SI), the strongest relative binding energy complex CBC-5C (**19a**):6KQI (MMGBSA dG Bind (NS)=-75.939 kcal/mol: Table 4-SI) and four interactions with the amino acid residues of 6KQI protein in the binding pocket as shown in the 2D and 3D diagrams of Figure 19.

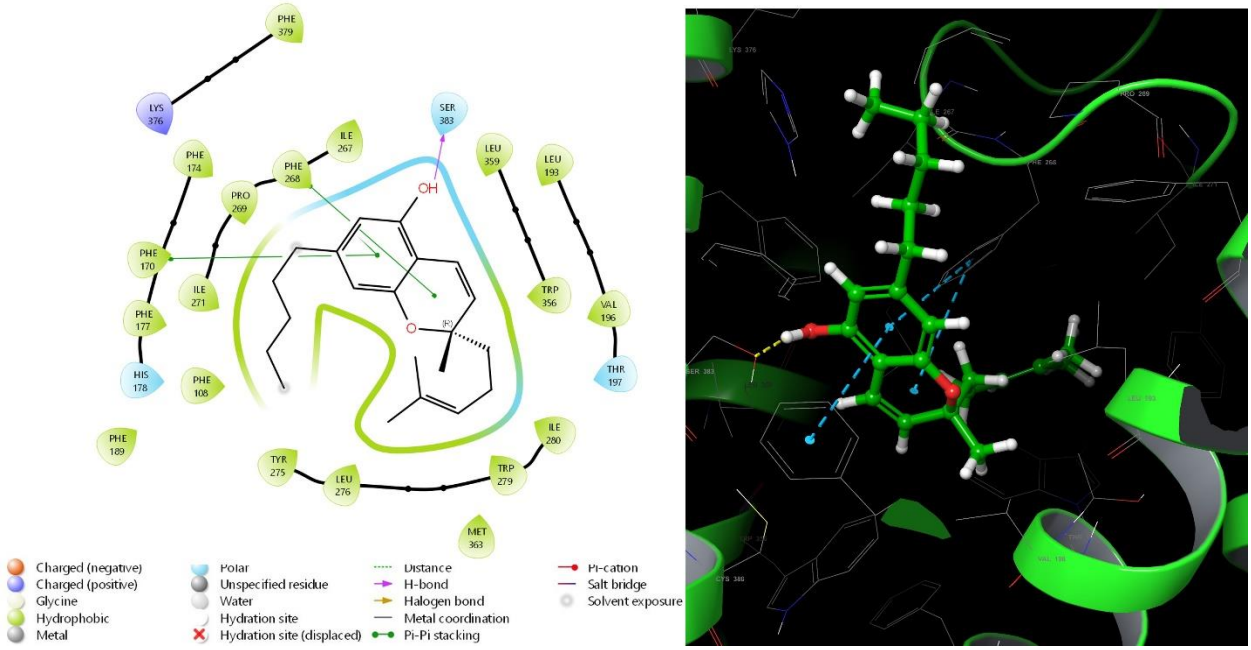

Figure 19: 3D and 2D diagrams of interactions of compound **19** with 6KQI where yellow dotted lines represent the H-bond and blue dotted line represents the π- π stacking interaction in the 3D diagram.

Previous mutagenesis studies have established Phe170, Phe268, Leu193, and Ser383 as essential amino acids for the binding of THC analogs or related agonists such as CP55940. These amino acids interact or are close to the preferred docking pose of the ligand [44].

The results of the docking with 6KPC protein which E3R agonist bound CB2 receptor displayed that 29 of the 44 docked cannabinoids showed good docking affinity in the binding pocket of 6KPC protein having a docking score in the range of -6.912 (compound **21**) to -10.557 (compound **28**). The most relevant amino acids in the binding pocket that interact with the

aromatic ring and phenolic groups of cannabinoids are Phe87, Phe183, Thr194 via π- π stacking bond and Ser285, Ile110, Thr114 via H-bond.

H_4CBD-adamantyl (**2b**, **2c**, **2d**), H_4CBD-3C (**4d**), CBD- adamantyl (**8b**), CBD-3C (**10b**, **10f**), CBD-5C (**11b**), THCBG (**13b**), THCBG -adamantyl (**14b**), THCBC -5C (**15_1a**), CBG-3C (**17**), CBG-5C (**17_1**), CBG-adamantyl (**18**), HHC-1C (**21c**, 2**1d**), HHC-adamantyl (**22c**), HHC-3C (**24d**, **24f**, **24g**), HHC-5C (**25c**, **25f**), D^9THC-adamantyl (**28f**), D^9THC-3C (**30a**, **30b**), D^9THC-5C (**31b**, **31c**), D^8THC-1C (**33a**, **33c**, **33d**), D^8THC-3C (**36b**, **36c**, **36d**), and CBN-7C (**40**) exhibited multiple interactions with the residues of 6KPC protein and good relative binding energies ligand: 6KPC (in the range of -52.082 kcal/mol to -79.316 kcal/mol). The most promising cannabinoids to bind with 6KPC protein are H_4CBD-adamantyl (**2**), and D^9THC-adamantyl (**28**) for presenting the best docking scores (-9.331, -10.557: Table 3-SI), the strongest relative binding energies (MMGBSA dG Bind (NS): 79.316 kcal/mol, -79.147 kcal/mol, respectively: Table 4-SI), and interacting with Phe 183, Phe 87 and Ser 285 amino acids in the binding pocket of the 6KPC protein via π- π stacking bond and H-bond (Figure 20).

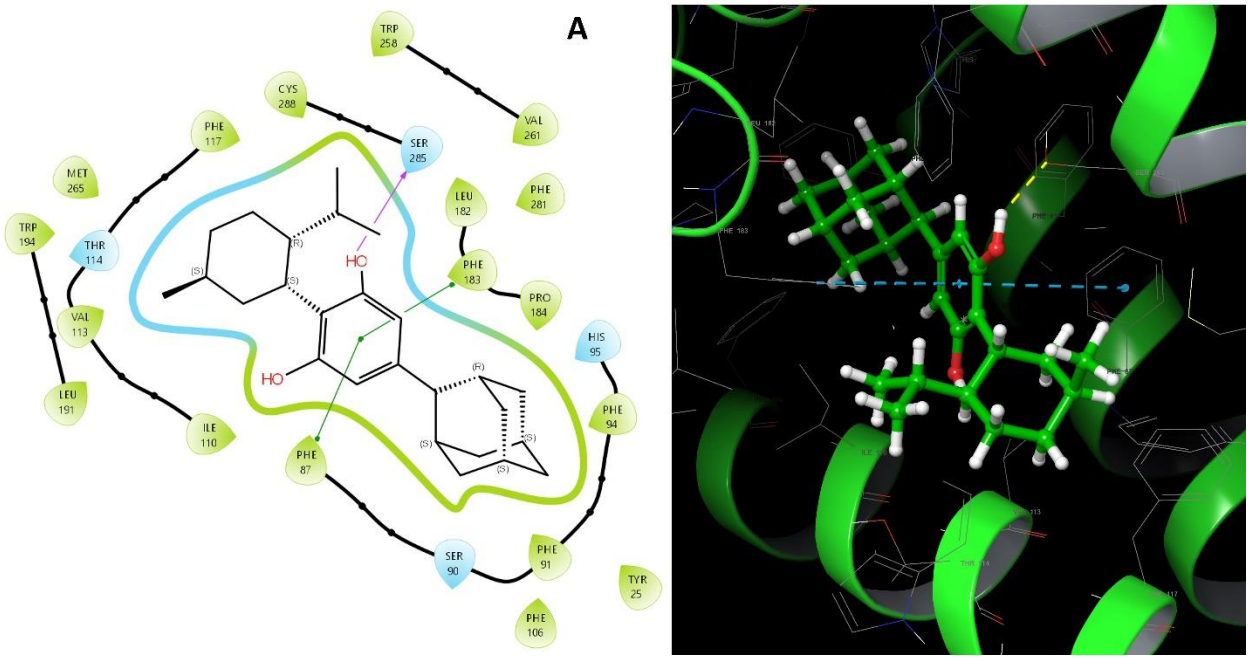

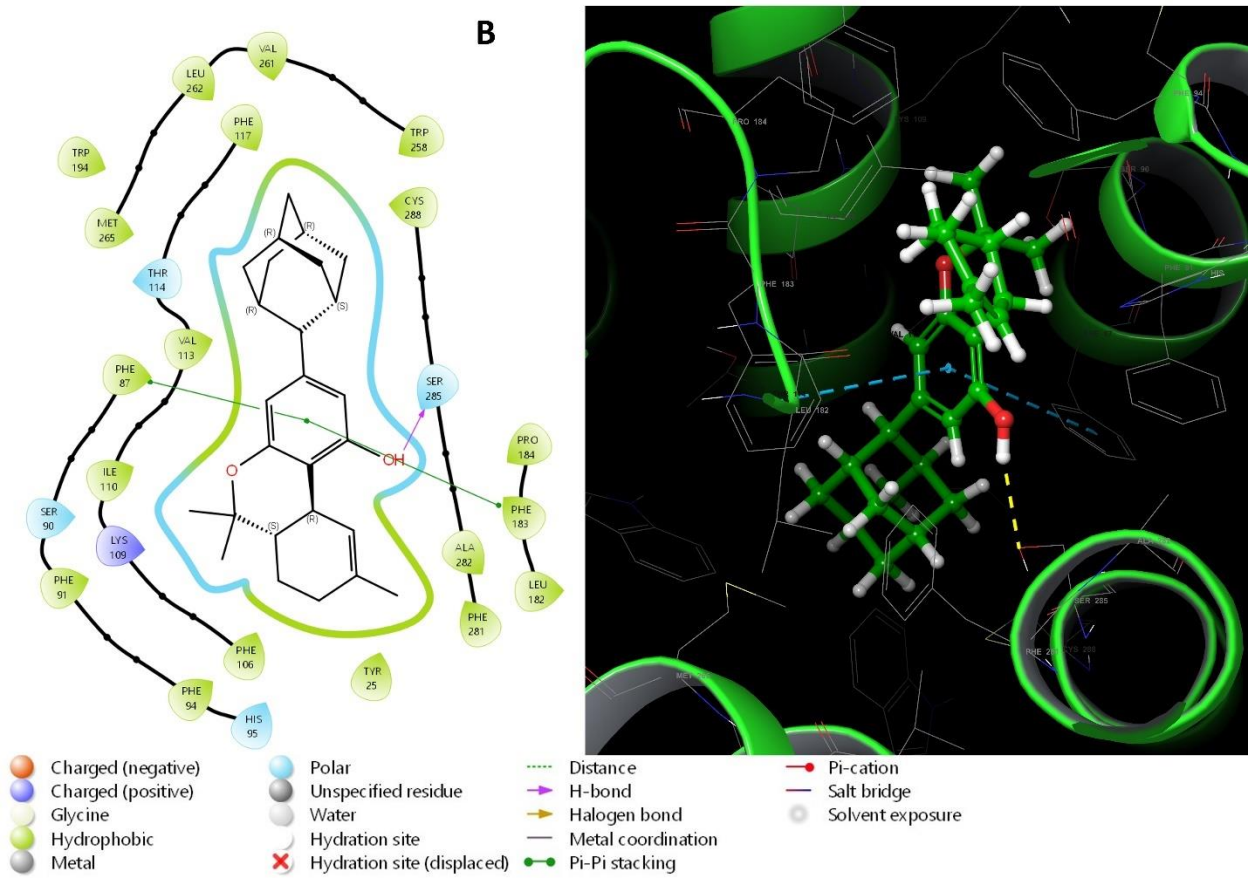

Figure 20: 3D and 2D diagrams of interactions of compounds **2** (A) and **28** (B) with 6KPC where yellow dotted lines represent the H-bond and blue dotted line represents the π- π stacking interaction in the 3D diagram.

The docking studies of 44 cannabinoids with 6PTO, a G*i* signaling complex bound with an agonist WIN 55,212-2 of the CB2 receptor revealed that 17 of the docked cannabinoids interact with Phe183 and Trp194 through hydrophobic interaction. In addition, they exhibited interactions through hydrogen bonds with Thr114, Ser285, and Ile110. These interactions are similar to those shown by the well-known WIN 55,212-2-CB2 agonist. The compounds that stood out with more interacting groups and stronger included H_4CBD-adamantyl (**2a**, **2b**, **2g**), CBG-3C (**17**), CBG-5C (**17_1**), HHC-1C (**21a**,**21b**,**21d**, **21e**), HHC-3C (**24a**, **24d**, **24e**), D^{9}THC-1C (**27c**), D^{9}THC-5C (**31c**), D^{8}THC-1C (**33c**), and D^{8}THC-3C (**36d**) (Figure 6-SI, Table 2-SI, Table 4-SI). These cannabinoids presented a docking score ranging between -5.033 (CBG-C3) and -9.529 (CBG-C5) (Table 3-SI). D^{8}THC-3C: 6PTO complex presented -77.056 kcal/mol, the

strongest MMGBSA dG Bind (NS) among the docked cannabinoids and interact with three residues of 6PTO protein: Trp194, Phe183 through π- π stacking bond and Ile110 via and H-bond as shown 2d and 3D diagrams of Figure 21.

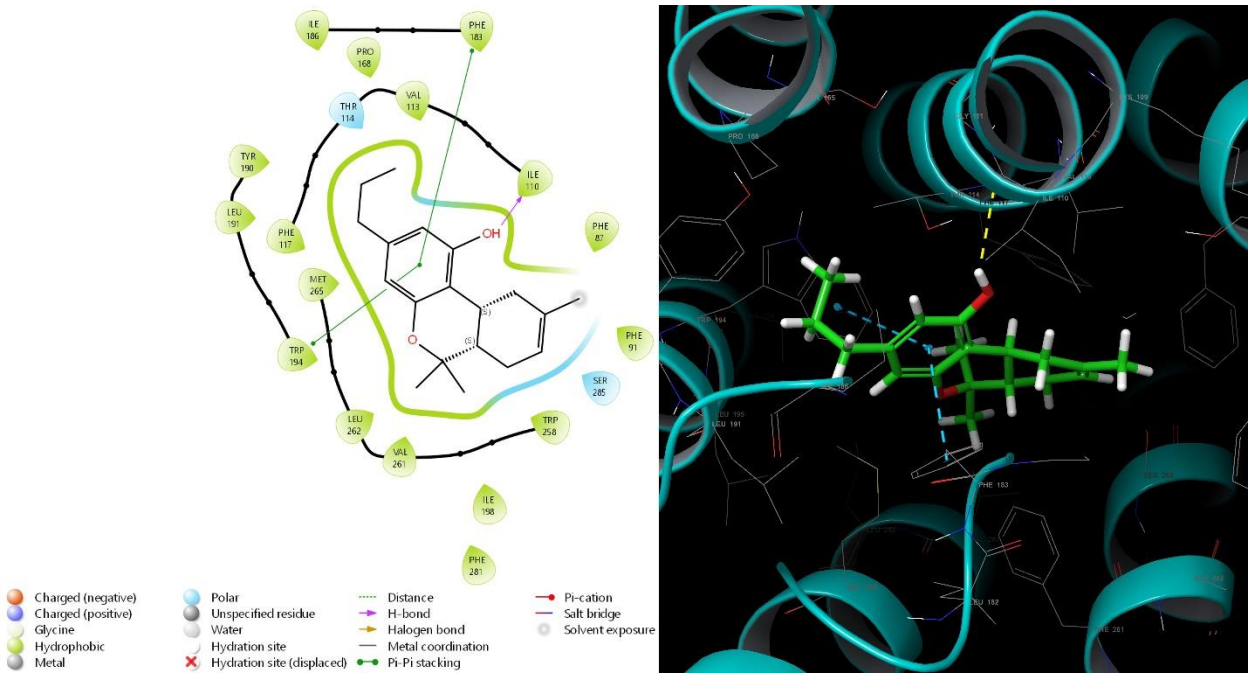

Figure 21: 3D and 2D diagrams of interactions of compound **36d** with 6PTO where yellow dotted lines represent the H-bond and blue dotted line represents the π- π stacking interaction in the 3D diagram.

Ross and et. al. [45] reported Org27569 as the first negative allosteric modulator of CB1. Although this compound was not approved by the FDA as a drug, has been used as a model to distinguish the allosteric site showing an uncommon complex allosteric profile at CB1. We carried out the docking study of cannabinoids using the protein 7V3Z as a CB1 receptor with a negative allosteric modulator ORG27569 bound. The specific interactions among the docked cannabinoids and 7V3Z residues are disclosed in Figure 8-SI and Table 2-SI. The cannabinoids: 7V3Z complexes that presented good affinity in the binding pocket with relative binding energies higher than 60 kcal/mol and the highest docking score (-6.981 to -10.821) involve H_4CBD-7C (**6b**), CBD-adamantyl (**8c**), CBD-3C (**10c**, **10e**), CBD-5C (**11c**), THCBG -5C (**13a**), THCBC -3C (**15a**). THCBC -5C (**15_1a**), THCBC -adamantyl (**16a**), CBG_5C (**17_1**), CBC-5C (**19**), HHC-

adamantyl (**22c**), HHC-7C (**26c**), D⁹THC-5C (**31b**, **31d**), and CBN-7C (**44**). In addition, the most important amino acids found in the binding pocket that interact with cannabinoids include Phe170, Phe268 via π- π stacking, and Ser505 via H-bond (Figure 22). It is interesting to note that THCBC -adamantyl (**16**) was the ligand with the strongest relative binding energy at -86.054 kcal/mol (Table 4-SI).

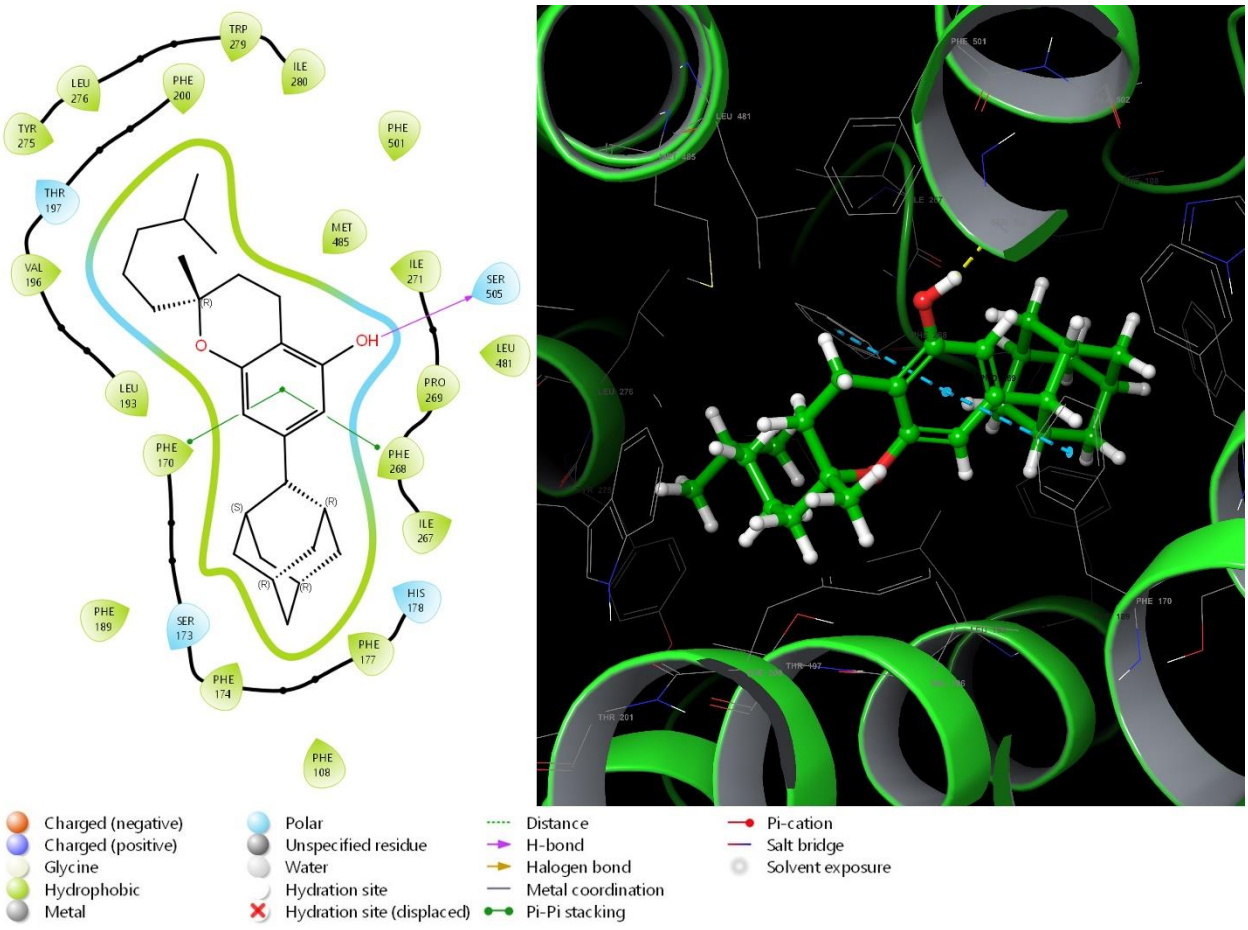

Figure 22: 3D and 2D diagrams of interactions of compound **16** with 7V3Z where yellow dotted lines represent the H-bond and blue dotted line represents the π- π stacking interaction in the 3D diagram.

Considering the docking study carried out using different models of CB1 and CB2 receptors, we demonstrated that the aromaticity of resorcinol moiety is essential for robust hydrophobic π–π stacking with amino acid residues establishing the deep binding pocket of the CB1 and CB2 receptors. For the three models of CB1 receptor, these residues are Phe170, Phe 268, and Trp279,

444 which are stationed neighboring the resorcinol ring of the tested compounds. However, Phe87,
445 Phe183, and Trp194 of the CB2 receptor bend to and make stable the ligand binding through π–π
446 stacking interactions with the phenolic ring-A of cannabinoids. In both CB receptors, the
447 hydrophobic interactions principally contribute to the good docking affinity.
448 The aromatic hydroxyl groups at the resorcinol ring have an essential function for the CB1 and
449 CB2 receptor activity. Huffman and et. al. [46] reported that the substitute of the phenolic
450 hydroxyl group in THC derivatives drastically reduces the CB1 activity. Our docking
451 experiments exposed the role of the hydroxyl groups in the interactions with the amino acids in
452 the binding pocket. For CB1 most of the cannabinoids presented hydrogen bonds between OH
453 groups in ring A with Ser383, or Ser505, which are key interacting residues for the CB1 affinity
454 [47, 48]. For CB2, the cannabinoids that were docked presented phenolic group interactions with
455 Ser285, Ile110, and/or Thr114 via hydrogen bonds. These bindings may stabilize the π-π stacking
456 interaction with Trp194 (Figures 4-, 6-, 7-SI) [49].
457 **GPR119 (7WCM)**
458 MBX-2982 is bound to 7WCM as an agonist of GPR119. Agonists that selectively activate
459 GPR119 can be used for the treatment of metabolic disorders [50,51]. In this work, we docked 44
460 cannabinoids into 7WCM protein to investigate the effectiveness of the binding of cannabinoids
461 with GPR119. Figure 9-SI and Table 2-SI display that CBD-1C (**7b**), THCBC -5C (**15_1a**),
462 CBG_3C (**17**), CBG_5C (**17_1**), HHC-1C (**21c**, **21e**) HHC-4C (**24g**), HHC-5C (**25c**), HHC-7C
463 (**26c**) have multiple interactions with the amino acids of 7WCM protein, the docking scores for
464 these cannabinoids are highest than -7.233 (Table 3-SI), and the relative binding energies of the
465 complexes ranging between -44.477 kcal/mol (HHC-1C (**21**): 7WCM) and -68.485 kcal/mol
466 (THCBC -5C (**15_1a**): 7WCM) as displayed Table 4-SI. The most typical interactions are π- π

467 stacking with Trp265 and Phe241 and hydrogen bonds with Val85 and Gluc261. Figure 23
468 exhibits the 2D (A, C) and 3D (B, C) ligand interaction diagram of THCBC -5C (**15_1a**) and
469 HHC-7C (**26c**). Considering this study, THCBC and HHC analogs presented strong relative
470 binding energies as well as multiple interactions in the binding pocket and hence may be possible
471 candidates to treat diabetes.

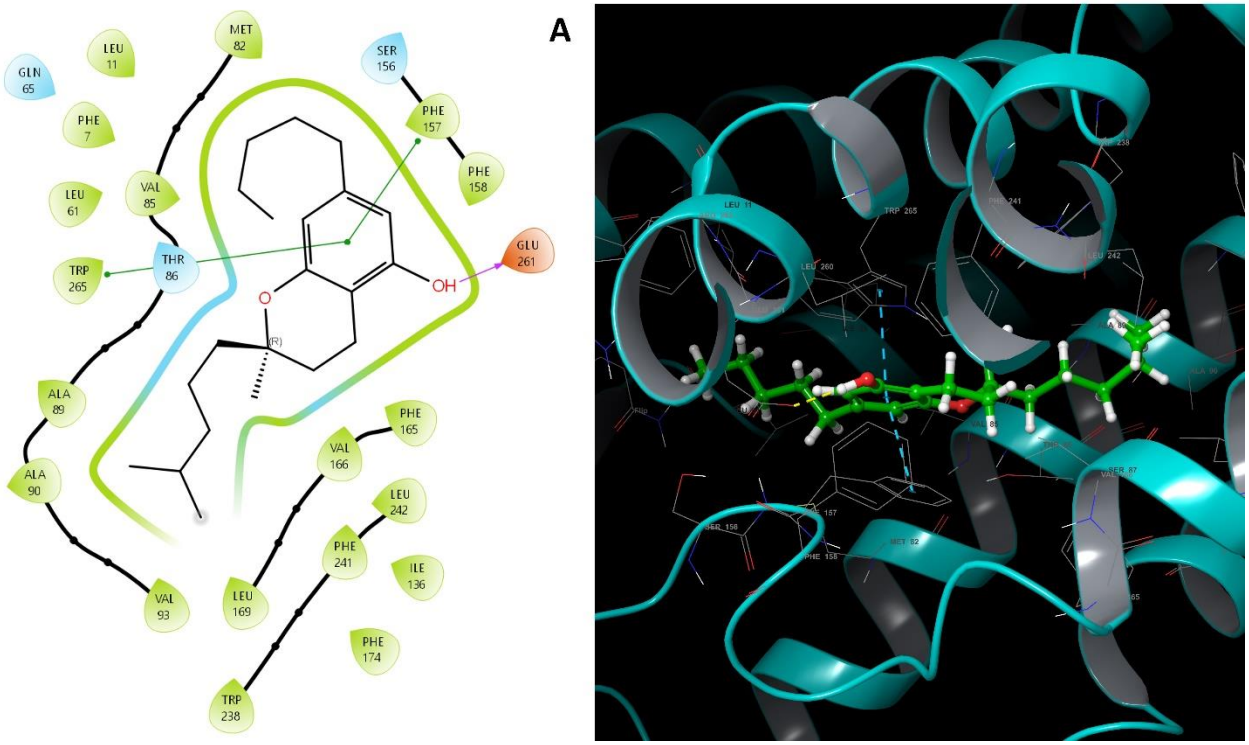

472

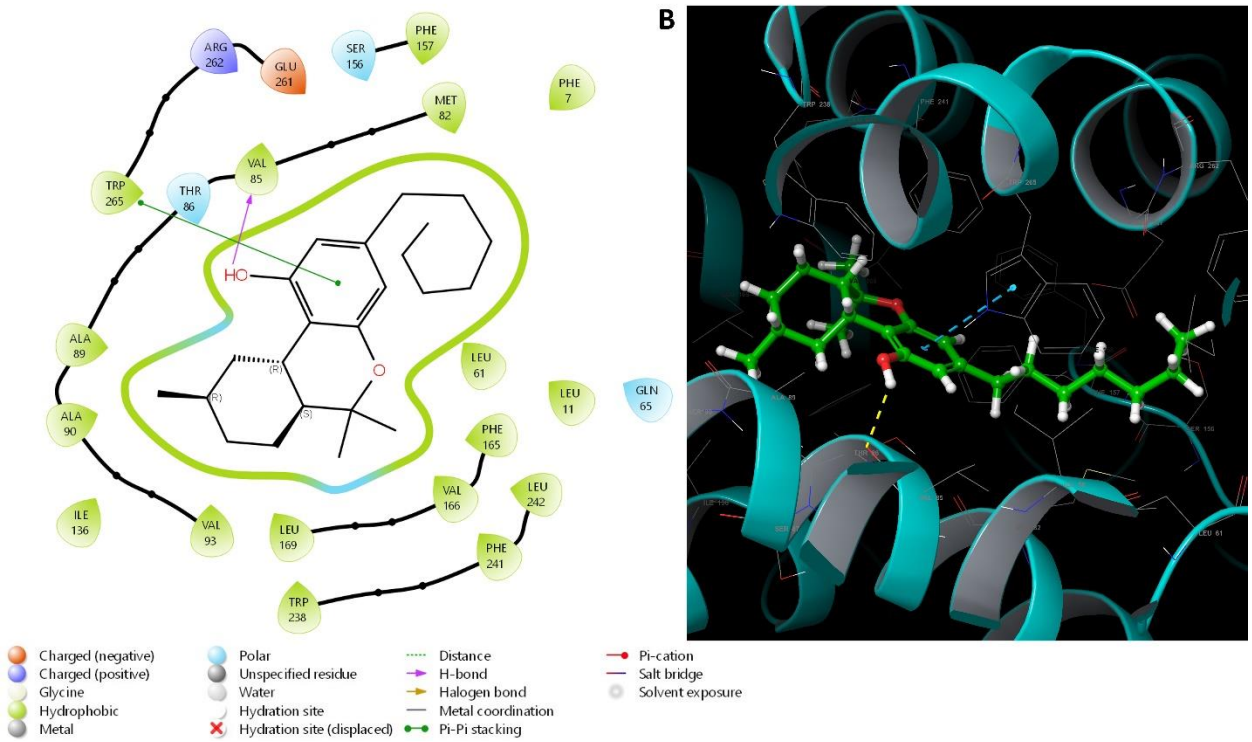

Figure 23: 3D and 2D diagrams of interactions of compounds **15_1** (A) and **26c** (B) with 7WCM where yellow dotted lines represent the H-bond and blue dotted line represents the π- π stacking interaction in the 3D diagram.

TRPV2 (8SLX)

Cannabinoids have been reported for the treatment of pain, but their mechanism has not been described yet. The inhibition of the TRPV1 and TRPV1 receptors is one of the possible targets for some of the biological activity of CBD and its analogs [52-54]. We reported a docking study with different types of cannabinoids with 8SLX protein (Rat TRPV2 bound with CBD ligand in nanodiscs). H_4CBD-1C (**1a**), H_4CBD-5C (**5c**), H_4CBD-7C (**6b**), CBD-7C (**7a**), THCBG -5C (**13b**), CBG-5C (**17_1**), and D^8THC-1C (**33a**) were the cannabinoids that exhibited good affinity in the binding pocket as shown in Figure 10-SI and Table 2-SI. Hydrophobic interactions type π-π stacking are the most relevant interactions with Phe540, and Tyr544 residues. Also, hydrogen bond interactions were found with Leu537 and Leu631 amino acids.

3.2. In Silico ADME Properties of Cannabinoids

Since lack of efficacy and safety are some of the most frequent causes of why a compound does not become an approved drug, the absorption, distribution, metabolism, and excretion (ADME) properties should be evaluated in the early stage of drug development. The drug-likeness and physiochemical properties of cannabinoids with docking affinity were analyzed via Maestro's QikProp Schrodinger software [55]. The predicted ADMET properties and descriptors for the compounds are presented in Table 5-SI. Some cannabinoids have solubility values out of the recommended range (compounds **2**, **6**, **8**, **13**, **14**, **16**, **19**, **20**, **22**, **23**, **25**, **26**, **28**, **31**, **37**, **38**, **40**, **44**). The solubility of cannabinoids is a challenge due to their lipophilic character. Cannabinoids with longer alkyl chains displayed poor solubility. Most other descriptors are within the recommended range by QikProp for 95% of known oral drugs. These results suggest that some of the tested cannabinoids exhibited acceptable physiochemical properties.

3.3 In silico identification of metabolic sites of cannabinoids using cytochrome P450

Herein, we report *in silico* study of cytochrome P450 (CYP-enzymes)-mediated metabolic of 44 cannabinoids that were docked previously. CYPs are one the most critical enzymes in drug metabolism and therefore of importance in clinical pharmacokinetics.

In the drug discovery process, an early estimate of potential metabolites allows time and resources to be reduced by removing drug candidates that present toxic metabolites.

Using Schrodinger software, we determined the possible sites of interactions between cannabinoids and P-450 to estimate the most likely metabolites, therefore supporting the comprehension of the structural changes needed to achieve ideal metabolic stability. The results are shown in Figure 11-SI.

Considering the oxidative metabolism of natural cannabinoids by cytochrome P450, we only found data for HHC, D^9-THC, CBD, CBC, CBG, and CBN [56]. Watanabe [57] and later Anderson [58] and Sarlah [59] determined the major oxidized metabolites of these cannabinoids (Figure 15). Hydroxylation, epoxidation, and quinone formation were the most typical reactions catalyzed by the P450 enzyme. The identified metabolites coincide with the oxidation active sites that were determined in the *in-silico* study. The hydroxylation of tricyclic cannabinoids (HHC, THC, and CBN) is carried out on the C-11 and C8. Also, it occurs at the first carbon of the lipophilic chain except for CBN. The hydroxylation of bicyclic cannabinoids (H_4CBD and CBD) was accomplished at C6 on the terpene moiety, C10 on the propenyl group, and C1 of the aliphatic chain of resorcinol ring. Finally, in the CBG and CBC analogs hydroxylation occurs in some CH_2 carbons at the allylic chain of the molecule and the epoxidation takes place at the double bond of the allylic chain. In the case of CBG, Sarlah [59] demonstrated that after the [2,3] epoxidation, undergo the intramolecular cyclization to obtain the tetrahydrofuran ring attached to the resorcinol core (**62**). The quinone formation is achieved in the resorcinol ring.

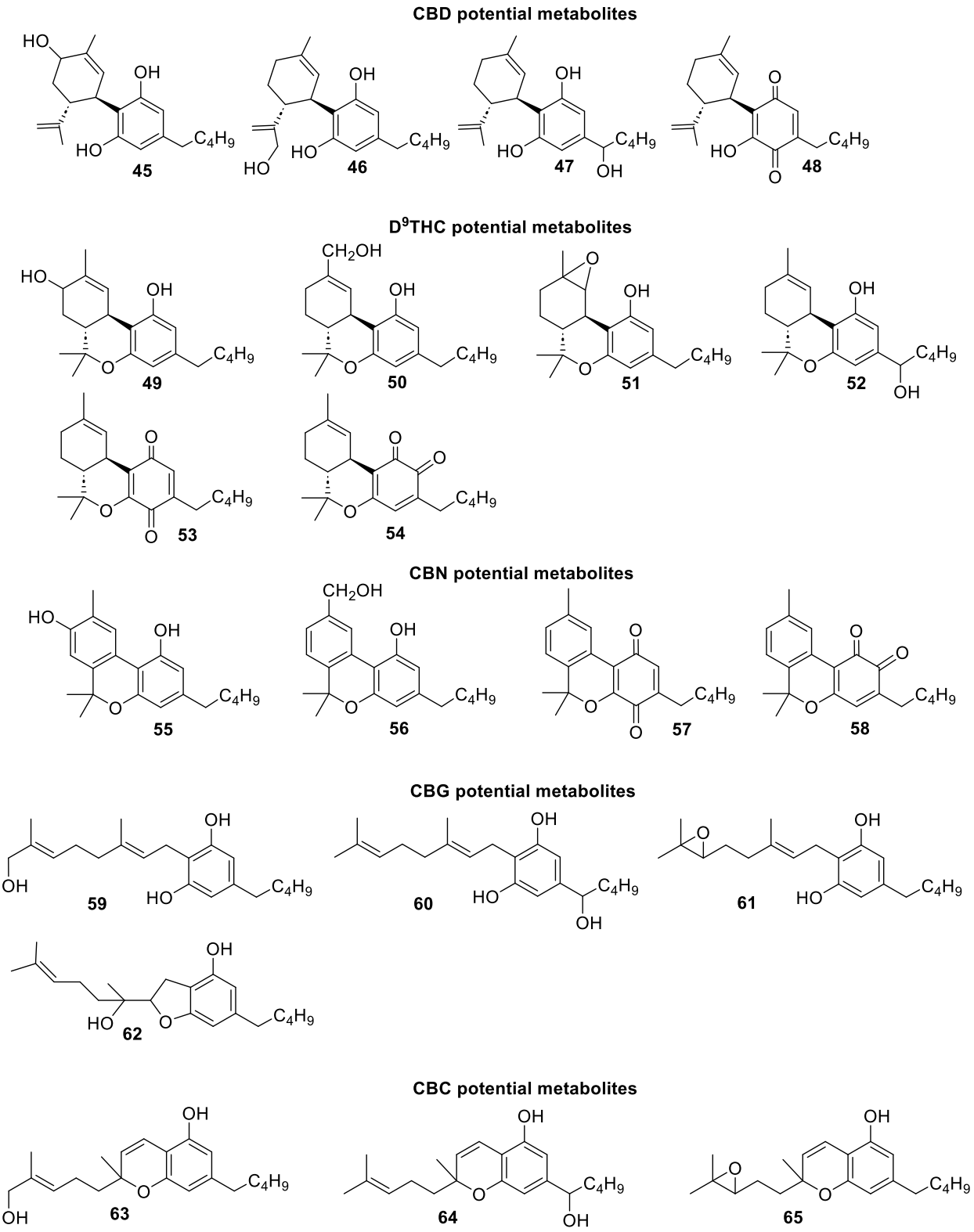

Figure 15: Potential oxidized metabolites of CBD, D^{9}THC, CBN, CBG, and CBC in the presence of the cytochrome P450.

529 The complex of 9L: 5U6B was found with -63.302 prime/mmgbsa dg bind energy and was good
530 than complexes with standards
531
532 **Conclusion**
533 The virtual screening residue-ligand interaction studies of saturated and unsaturated
534 cannabinoids using different types of CB1 and CB2 receptors PPAR-γ, GPR119, and TRPV2
535 models showed the relevance of some amino acids in the binding pocket as well as the
536 importance of the hydrogen bond, and hydrophobic interactions among cannabinoids and the
537 residues. The most promising cannabinoids considering docking scores, relative binding
538 energies, and multiple interactions with the protein in the binding pocket are D^9THC-1C (**27b**)
539 with 2P4Y, CBN-7C (**44**) with 5DFP, CBG-5C (**17_1**) with 5UO9, HHC-1C (**21e**) with 5ZTY,
540 CBC-5C (**19**) with 6KQI, H_4CBD-adamantyl (**2**) and D^9THC-adamantyl (**28**) with 6KPC, D^8THC-
541 3C (**36d**) with 6PTO, THCBC -adamantyl (**16**) with 7V3Z, THCBC -3C (**15_1**) and HHC-7C
542 (**26c**) with 7WCM. The physiochemical properties of each cannabinoid were also measured,
543 demonstrating that almost all the calculated properties of the compounds are within the ranges
544 projected except those cannabinoids with more than 3 carbons in the lipophilic chain present
545 poor aqueous solubility. Related to the *in-silico* study of the oxidative metabolism of
546 cannabinoids by cytochrome P450, we conclude that all cannabinoids displayed similar sites of
547 reported interactions with CYP enzymes.
548
549 **Abbreviations**
550 ADME - Adsorption, distribution, metabolism, excretion
551 Arg – Arginine

552 Asp – Aspartic Acid

553 CBC – Cannabichromene

554 CBCA – Cannabichromenic acid

555 CBD – Cannabidiol

556 CBDA – Cannabidiolic acid

557 CBG – Cannabigerol

558 CBGA – Cannabigerolic acid

559 CBR – Cannabinoid Receptor

560 Cys – Cystine

561 DFT – Density Funtional Theory

562 GC-MS - Gas chromatography-Mass spectrometry

563 Glu – Glutamic acid

564 H_4CBD – Hexahydrocannabidiol

565 H-bonding – Hydrogen bonding

566 HHC – Hexahydrocannabinol

567 HHCV - hexahydrocannabivarin

568 His – Histidine

569 IC50 – Half-maximal inhibitory concentration

570 Ile – Isoleucine

571 Leu – Leucine

572 Met – Methionine

573 MTT - 3-[4,5-dimethylthiazol-2-yl]-2,5-diphenyltetrazolium bromide

574 NAM – Negative allosteric modulator

PAM – Positive allosteric modulator

PDB – Protein database

Phe – Phenylalanine

RCSB – Research Collaboratory for Structural Bioinformatics

RMSD – Root mean square deviation

Ser – Serine

THC – Tetrahydrocannabinol

THCA – Tetrahydrocannabinolic acid

THCBC – Hydrogenated CBC

THCBG – Hydrogenated CBG

THCV – Tetrahydrocannabivarin

Thr – Threonine

TMSCl – Chlorotrimethylsilane

Trp –Tryptophan

Tyr –Tyrosine

Val – Valine

Author Information

ORCID

Maite L. Docampo-Palacios: https://orcid.org/0000-0001-5205-3989

Giovanni Ramirez: https://orcid.org/0000-0002-3716-862X

Tesfay Tesfatsion: https://orcid.org/0000-0002-3743-9522

598 Monica Pittilgio: https://orcid.org/0009-0007-1044-7614

599 Kyle Ray: https://orcid.org/0000-0001-5648-0099

600 Westley Cruces: https://orcid.org/0000-0003-3023-7626

601

602 **Author Contributions:** Conceptualization: MLD, GAR, WC. Methodology: GAR, WC. Data

603 Analysis: MLD, GAR, TTT, WC. Computational Modeling: GAR. Writing – Original Draft:

604 MLD, GAR, WC. Writing – Revision and Editing: MLD, GAR, TTT, MKP, WC. Supervision:

605 WC. Project Administration: KPR, WC.

606

607 **Author Confirmation:** All authors have read and approved this manuscript for submission.

608

609 **Author Disclosure:** MLD, GAR, TTT, and MKP are employees of Colorado Chromatography

610 Labs. WC and KPR are founders of Colorado Chromatography Labs.

611

612 **Funding Statement:** There is no funding to report.

613

614 **References**

615 1. Hachem, M., Alkuwaildi, B., Tamim, F. B., Altamimi, M. J. Emergence of

616 Hexahydrocannabinol as a psychoactive drug of abuse in e-cigarette liquids,

617 https://doi.org/10.21203/rs.3.rs-3047132/v1

618 2. Ujuary, I. Hexahydrocannabinol, and closely related semi-synthetic cannabinoids: a

619 comprehensive review, *Drug Testing and Analysis*, **2023**, https://doi.org/10.1002/dta.3519

3. Geci M, Scialdone M, Tishler J. The dark side of cannabidiol: The unanticipated social and clinical implications of synthetic Δ8-THC. *Cannabis Cannabinoid Res*. **2023**;8(2):270–82. http://dx.doi.org/10.1089/can.2022.0126

4. Erickson, B. E., Delta-8-THC craze concerns chemists, *Chemistry & Engineering News*, **2021**, 99, 31, https://cen.acs.org/biological-chemistry/natural-products/Delta-8-THC-craze-concerns/99/i31

5. Adams R. Marihuana active compounds. US2419937 patent issued 6 May 1947

6. Docampo-Palacios, M. L.; Ramirez, G. A.; Tesfatsion, T. T.; Okhovat, A.; Pittiglio, M.; Ray, K. P.; Cruces, W. Saturated Cannabinoids: Update on Synthesis Strategies and Biological Studies of These Emerging Cannabinoid Analogs. *Molecules* **2023**, *28* (17), 6434. https://doi.org/10.3390/molecules28176434.

7. Ben-Shabat, S., Hanus, L. O., Katzavian, G., & Gallily, R. New cannabidiol derivatives: synthesis, binding to cannabinoid receptor, and evaluation of their antiinflammatory activity. *Journal of Medicinal Chemistry*, **2006**, 49(3), 1113–1117. https://doi.org/10.1021/jm050709m

8. Scialdone MA. Hydrogenation of cannabis oil. United States Patent. 2018; US 10,071,127 B2

9. Collins, A.; Ramirez, G.; Tesfatsion, T.; Ray, K. P.; Caudill, S.; Cruces, W. Synthesis and Characterization of the Diastereomers of HHC and H4CBD. *Nat. Prod. Commun.* **2023**, *18* (3), 1934578X2311589. https://doi.org/10.1177/1934578x231158910.

10. Collins, A.C; Ray, K.P; Cruces, W. A method for preparing hexahydrocannabinol. US patent 63/411,506, 29 September 2022

11. Collins, A., Tesfastion, T., Ramirez, G., Ray, K., and Cruces, W. Nonclinical In Vitro Safety Assessment Summary of Hemp Derived (R/S)-Hexahydrocannabinol ((R/S)-HHC),

643 *Cannabis Science and Technology*® **2022**, 5(7), 23-27. https://doi.org/10.21203/rs.3.rs-
644 2299264/v1
645 12. Tesfatsion, T. T.; Ramirez, G. A.; Docampo-Palacios, M. L.; Collins, A. C.; Ray, K. P.;
646 Cruces, W. Evaluation of Preclinical *in Vitro* Cytotoxicity, Genotoxicity, and Cardiac-Toxicity
647 Screenings of Hydrogenated Cannabidiol. *Pharmacogn. Mag.* **2023**.
648 https://doi.org/10.1177/09731296231195941.
649 13. Skinner WA, Rackur G, Uyeno E. Structure-activity studies on tetrahydro- and
650 hexahydrocannabinol derivatives. J Pharm Sci. 1979;68(3):330–2.
651 http://dx.doi.org/10.1002/jps.2600680319
652 14. Harvey, D. J., Brown, N. K., In vitro metabolism of cannabigerol in several mammalian
653 species, *Biomedical and Environmental Mass Spectrometry*, **1990**, 19, 545-553.
654 https://doi.org/10.1002/bms.1200190905
655 15. Harvey, D. J., Brown, N. K., A method for the structural determination of
656 canabichromene metabolites by mass spectrometry, *Rapid Communications in Mass*
657 *Spectrometry*, **1990**, 4 (4), 135-136. https://doi.org/10.1002/bms.1200190905
658 16. ElSohly, H. N., Turner, C. E., Clark, A. M., ElSohly, M. A., Synthesis and antimicrobial
659 activities of certain cannabichromene and cannabigerol related compounds, *Journal of*
660 *Pharmaceutical Sciences*, **1982**, 71 (12), 1319-1323.Https://doi.org/10.1002/jps.2600711204.
661 17. (Scheme 3) Tahir, M. N.; Shahbazi, F.; Rondeau-Gagné, S.; Trant, J. F. The Biosynthesis
662 of the Cannabinoids. *J. Cannabis Res.* **2021**, *3* (1). https://doi.org/10.1186/s42238-021-00062-4.
663 18. Tesfatsion, T. T., Ramirez, G. A., Docampo-Palacios, M. L., Collins, A. C., Mzannar, Y.,
664 Khan, H. Y., Aboukameel, O., Azmi, A. S., Jagtap, P. G., Ray, K. P., Cruces, W. Antineoplastic
665 Properties of THCV, HHC and their anti-Proliferative effects on HPAF-II, MIA-paca2, Aspc-1,

and PANC-1 PDAC Pancreatic Cell Lines, **2022**, S*ubmitted,* Preprint: https://doi.org/10.26434/chemrxiv-2022-v4zqc

19. Thapa, D.; Lee, J. S.; Heo, S.-W.; Lee, Y. R.; Kang, K. W.; Kwak, M.-K.; Choi, H. G.; Kim, J.-A. Novel Hexahydrocannabinol Analogs as Potential Anti-Cancer Agents Inhibit Cell Proliferation and Tumor Angiogenesis. *Eur. J. Pharmacol.* **2011**, *650* (1), 64–71. https://doi.org/10.1016/j.ejphar.2010.09.073

20. Aviz-Amador, A.; Contreras-Puentes, N.; Mercado-Camargo, J. Virtual Screening Using Docking and Molecular Dynamics of Cannabinoid Analogs against CB1 and CB2 Receptors. *Comput. Biol. Chem.* **2021**, *95* (107590), 107590. https://doi.org/10.1016/j.compbiolchem.2021.107590.

21. Thapa, D.; Babu, D.; Park, M.-A.; Kwak, M.-K.; Lee, Y.-R.; Kim, J. M.; Kwon, T. K.; Kim, J.-A. Induction of P53-Independent Apoptosis by a Novel Synthetic Hexahydrocannabinol Analog Is Mediated via Sp1-Dependent NSAID-Activated Gene-1 in Colon Cancer Cells. *Biochem. Pharmacol.* **2010**, *80* (1), 62–71. https://doi.org/10.1016/j.bcp.2010.03.008.

22. Docampo-Palacios, M. L., Tesfatsion, T. T., Ramirez, G. A. Jagtap, P. G., Ray, K. P., Cruces, W. Cytotoxic Cannabinoid Analogs for the Treatment of Pancreatic Ductal Adenocarcinoma Cancer, *In Proceedings of the ACS Fall 2023: Harnessing the Power of Data, San Francisco, CA, USA*, 10–13 June **2023** (oral presentation). https://doi.org/10.1021/scimeetings.3c10038.

23. Ramirez, G. A. Tesfatsion, T. T., Jagtap, P. G., Ray, K. P., Cruces, W. Cytotoxic cannabinoid analogs for prevention of cancer, *In Proceedings of the ACS Spring 2023: Crossroads of Chemistry, Indianapolis, IN, USA*, 26–30 March **2023** (poster presentation) https://doi.org/10.1021/scimeetings.3c00071

24. Lovering, F.; Bikker, J.; Humblet, C. Escape from Flatland: Increasing Saturation as an Approach to Improving Clinical Success. *J. Med. Chem.* **2009**, *52* (21), 6752–6756. https://doi.org/10.1021/jm901241e.

25. Howlett, A. C.; Abood, M. E. CB 1 and CB 2 Receptor Pharmacology. In *Cannabinoid Pharmacology*; Elsevier, **2017**, 80, 169–206. https://doi:10.1016/bs.apha.2017.03.007.

26. An, D.; Peigneur, S.; Hendrickx, L. A.; Tytgat, J. Targeting Cannabinoid Receptors: Current Status and Prospects of Natural Products. *Int. J. Mol. Sci.* **2020**, *21* (14), 5064. https://doi.org/10.3390/ijms21145064.

27. Elbrecht, A.; Chen, Y.; Cullinan, C. A.; Hayes, N.; Leibowitz, M. D.; Moller, D. E.; Berger, J. Molecular Cloning, Expression and Characterization of Human Peroxisome Proliferator Activated Receptors Γ1 and Γ2. *Biochem. Biophys. Res. Commun.* **1996**, *224* (2), 431–437. https://doi.org/10.1006/bbrc.1996.1044.

28. Anand, K.; Nair, S. A.; Radhakrishna, P. M. Biology of PPARγ in Cancer: A Critical Review on Existing Lacunae. *Current Molecular Medicine*. **2007**, *7*(6), 532-540. Https://doi.org/10.2174/156652407781695765.

29. Kumar, R.; Gururaj, A. E.; Barnes, C. J. P21-Activated Kinases in Cancer. *Nat. Rev. Cancer* **2006**, *6* (6), 459–471. https://doi.org/10.1038/nrc1892.

30. Yang, Y.; Huynh, N.; Dumesny, C.; Wang, K.; He, H.; Nikfarjam, M. Cannabinoids Inhibited Pancreatic Cancer via P-21 Activated Kinase 1 Mediated Pathway. *Int. J. Mol. Sci.* **2020**, *21* (21), 8035. https://doi.org/10.3390/ijms21218035.

31. Grant, B. J.; Gorfe, A. A.; McCammon, J. A. Large Conformational Changes in Proteins: Signaling and Other Functions. *Curr. Opin. Struct. Biol.* **2010**, *20* (2), 142–147. https://doi.org/10.1016/j.sbi.2009.12.004.

32. Romero, L.; Caldero, F. A Tutorial on Parametric Image Registration. In *Scene Reconstruction Pose Estimation and Tracking*; Stolkin, R., Ed.; I-Tech Education and Publishing: London, England, **2007** https://www.intechopen.com/books/297.

33. Adhav, V. A.; Saikrishnan, K. The Realm of Unconventional Noncovalent Interactions in Proteins: Their Significance in Structure and Function. *ACS Omega* **2023**, *8* (25), 22268–22284. https://doi.org/10.1021/acsomega.3c00205.

34. . (Figure 9) Pisanti, S.; Picardi, P.; D'Alessandro, A.; Laezza, C.; Bifulco, M. The Endocannabinoid Signaling System in Cancer. *Trends Pharmacol. Sci.* **2013**, *34* (5), 273–282. https://doi.org/10.1016/j.tips.2013.03.003.

35. Das, S.; Kaul, K.; Mishra, S.; Charan, M.; Ganju, R. K. Cannabinoid Signaling in Cancer. In *Advances in Experimental Medicine and Biology*; Springer International Publishing: Cham, **2019**; pp 51–61. https://doi.org/10.1007/978-3-030-21737-2_4.

36. (Figure 10) Pagano, C.; Navarra, G.; Coppola, L.; Bifulco, M.; Laezza, C. Molecular Mechanism of Cannabinoids in Cancer Progression. *Int. J. Mol. Sci.* **2021**, *22* (7), 3680. https://doi.org/10.3390/ijms22073680.

37. Leijten-van de Gevel, I. A.; van Herk, K. H. N.; de Vries, R. M. J. M.; Ottenheym, N. J.; Ottmann, C.; Brunsveld, L. Indazole MRL-871 Interacts with PPARγ via a Binding Mode That Induces Partial Agonism. *Bioorg. Med. Chem.* **2022**, *68* (116877), 116877. https://doi.org/10.1016/j.bmc.2022.116877.

38. Yang, Y.; Huynh, N.; Dumesny, C.; Wang, K.; He, H.; Nikfarjam, M. Cannabinoids Inhibited Pancreatic Cancer via P-21 Activated Kinase 1 Mediated Pathway. *Int. J. Mol. Sci.* **2020**, *21* (21), 8035. https://doi.org/10.3390/ijms21218035.

734 39. van Aalst, E.; Wylie, B. J. Cholesterol Is a Dose-Dependent Positive Allosteric Modulator
735 of CCR3 Ligand Affinity and G Protein Coupling. *Front. Mol. Biosci.* **2021**, *8*.
736 https://doi.org/10.3389/fmolb.2021.724603.
737 40. López-Rodríguez, M. L.; Benhamú, B.; Vázquez-Villa, H. Allosteric Modulators
738 Targeting GPCRs. In *GPCRs*; Elsevier, 2020; pp 195–241.
739 41. Burford, N. T.; Livingston, K. E.; Canals, M.; Ryan, M. R.; Budenholzer, L. M. L.; Han,
740 Y.; Shang, Y.; Herbst, J. J.; O'Connell, J.; Banks, M.; Zhang, L.; Filizola, M.; Bassoni, D. L.;
741 Wehrman, T. S.; Christopoulos, A.; Traynor, J. R.; Gerritz, S. W.; Alt, A. Discovery, Synthesis,
742 and Molecular Pharmacology of Selective Positive Allosteric Modulators of the δ-Opioid
743 Receptor. *J. Med. Chem.* **2015**, *58* (10), 4220–4229.
744 https://doi.org/10.1021/acs.jmedchem.5b00007.
745 42. Abdel-Magid, A. F. Allosteric Modulators: An Emerging Concept in Drug
746 Discovery. *ACS Med. Chem. Lett.* **2015**, *6* (2), 104–107. https://doi.org/10.1021/ml5005365.
747 43. Wood, M. R.; Hopkins, C. R.; Brogan, J. T.; Conn, P. J.; Lindsley, C. W. "Molecular
748 Switches" on MGluR Allosteric Ligands That Modulate Modes of
749 Pharmacology. *Biochemistry* **2011**, *50* (13), 2403–2410. https://doi.org/10.1021/bi200129s.
750 44. Shao, Z.; Yin, J.; Chapman, K.; Grzemska, M.; Clark, L.; Wang, J.; Rosenbaum, D. M.
751 High-Resolution Crystal Structure of the Human CB1 Cannabinoid
752 Receptor. *Nature* **2016**, *540* (7634), 602–606. https://doi.org/10.1038/nature20613.
753 45. Price, M. R.; Baillie, G. L.; Thomas, A.; Stevenson, L. A.; Easson, M.; Goodwin, R.;
754 McLean, A.; McIntosh, L.; Goodwin, G.; Walker, G.; Westwood, P.; Marrs, J.; Thomson, F.;
755 Cowley, P.; Christopoulos, A.; Pertwee, R. G.; Ross, R. A. Allosteric Modulation of the

Cannabinoid CB_1 Receptor. *Mol. Pharmacol.* **2005**, *68* (5), 1484–1495. https://doi.org/10.1124/mol.105.016162.

46. Huffman, J. W.; Yu, S.; Showalter, V.; Abood, M. E.; Wiley, J. L.; Compton, D. R.; Martin, B. R.; Bramblett, R. D.; Reggio, P. H. Synthesis and Pharmacology of a Very Potent Cannabinoid Lacking a Phenolic Hydroxyl with High Affinity for the CB2 Receptor. *J. Med. Chem.* **1996**, *39* (20), 3875–3877. https://doi.org/10.1021/jm960394y.

47. Chung, H.; Fierro, A.; Pessoa-Mahana, C. D. Cannabidiol Binding and Negative Allosteric Modulation at the Cannabinoid Type 1 Receptor in the Presence of Delta-9-Tetrahydrocannabinol: An In Silico Study. *PLoS One* **2019**, *14* (7), e0220025. https://doi.org/10.1371/journal.pone.0220025.

48. Ji, B.; Liu, S.; He, X.; Man, V. H.; Xie, X.-Q.; Wang, J. Prediction of the Binding Affinities and Selectivity for CB1 and CB2 Ligands Using Homology Modeling, Molecular Docking, Molecular Dynamics Simulations, and MM-PBSA Binding Free Energy Calculations. *ACS Chem. Neurosci.* **2020**, *11* (8), 1139–1158. https://doi.org/10.1021/acschemneuro.9b00696.

49. Li, X.; Chang, H.; Bouma, J.; de Paus, L. V.; Mukhopadhyay, P.; Paloczi, J.; Mustafa, M.; van der Horst, C.; Kumar, S. S.; Wu, L.; Yu, Y.; van den Berg, R. J. B. H. N.; Janssen, A. P. A.; Lichtman, A.; Liu, Z.-J.; Pacher, P.; van der Stelt, M.; Heitman, L. H.; Hua, T. Structural Basis of Selective Cannabinoid CB2 Receptor Activation. *Nat. Commun.* **2023**, *14* (1). https://doi.org/10.1038/s41467-023-37112-9.

50. Qian, Y.; Wang, J.; Yang, L.; Liu, Y.; Wang, L.; Liu, W.; Lin, Y.; Yang, H.; Ma, L.; Ye, S.; Wu, S.; Qiao, A. Activation and Signaling Mechanism Revealed by GPR119-Gs Complex Structures. *Nat. Commun.* **2022**, *13* (1). https://doi.org/10.1038/s41467-022-34696-6.

51. Xu, P.; Huang, S.; Guo, S.; Yun, Y.; Cheng, X.; He, X.; Cai, P.; Lan, Y.; Zhou, H.; Jiang, H.; Jiang, Y.; Xie, X.; Xu, H. E. Structural Identification of Lysophosphatidylcholines as Activating Ligands for Orphan Receptor GPR119. *Nat. Struct. Mol. Biol.* **2022**, *29* (9), 863–870. https://doi.org/10.1038/s41594-022-00816-5.

52. Anand, U.; Jones, B.; Korchev, Y.; Bloom, S. R.; Pacchetti, B.; Anand, P.; Sodergren, M. H. CBD Effects on TRPV1 Signaling Pathways in Cultured DRG Neurons. *J. Pain Res.* **2020**, *13*, 2269–2278. https://doi.org/10.2147/jpr.s258433.

53. Starkus, J.; Jansen, C.; Shimoda, L. M. N.; Stokes, A. J.; Small-Howard, A. L.; Turner, H. Diverse TRPV1 Responses to Cannabinoids. *Channels (Austin)* **2019**, *13* (1), 172–191. https://doi.org/10.1080/19336950.2019.1619436.

54. Ghasemi-Gojani, E.; Kovalchuk, I.; Kovalchuk, O. Cannabinoids and Terpenes for Diabetes Mellitus and Its Complications: From Mechanisms to New Therapies. *Trends Endocrinol. Metab.* **2022**, *33* (12), 828–849. https://doi.org/10.1016/j.tem.2022.08.003.

55. Schrödinger, LLC . *Schrödinger Release 2021-4: QikProp.* Schrödinger, LLC; New York, NY, USA: 2021.

56. Zendulka, O.; Dovrtělová, G.; Nosková, K.; Turjap, M.; Šulcová, A.; Hanuš, L.; Juřica, J. Cannabinoids and Cytochrome P450 Interactions. *Curr. Drug Metab.* **2016**, *17* (3), 206–226. https://doi.org/10.2174/1389200217666151210142051.

57. Watanabe, K.; Yamaori, S.; Funahashi, T.; Kimura, T.; Yamamoto, I. Cytochrome P450 Enzymes Involved in the Metabolism of Tetrahydrocannabinols and Cannabinol by Human Hepatic Microsomes. *Life Sci.* **2007**, *80* (15), 1415–1419. https://doi.org/10.1016/j.lfs.2006.12.032.

58. Doohan, P. T.; Oldfield, L. D.; Arnold, J. C.; Anderson, L. L. Cannabinoid Interactions with Cytochrome P450 Drug Metabolism: A Full-Spectrum Characterization. *AAPS J.* **2021**, *23* (4). https://doi.org/10.1208/s12248-021-00616-7.

59. Roy, P.; Dennis, D. G.; Eschbach, M. D.; Anand, S. D.; Xu, F.; Maturano, J.; Hellman, J.; Sarlah, D.; Das, A. Metabolites of Cannabigerol Generated by Human Cytochrome P450s Are Bioactive. *Biochemistry* **2022**, *61* (21), 2398–2408. https://doi.org/10.1021/acs.biochem.2c00383.